Numerical simulation of the flow in a disc refiner

Gohar.M.Khokhar

KTH Engineering Sciences

Master of Science- Thesis
Engineering Mechanics
Stockholm, Sweden 2011

Preface

This thesis in fluid mechanics is the final degree project for the Master of Engineering Mechanics program at Royal Institute of Technology (KTH). This work has been carried out in department of Mechanics at Royal Institute of Technology (KTH) in cooperation with Innventia AB.

I am grateful to my supervisors Anders Dahlkild and Lisa Prahl from KTH-Mechanics, Ulla-Brit Mohlin and Magnus Björkman from Innventia AB for their guidance and support.

Gohar .M. Khokhar

Numerical simulation of the flow in a disc refiner

Gohar Khokhar

Degree project in Engineering Mechanics
Stockholm, Sweden 2011

Abstract

The thesis work is carried out in Innventia AB and Royal Institute of Technology (KTH). The objective of the study was to numerically simulate the flow inside the disc refiner and to determine the factors influencing the development of flow in the rotor and the stator of the disc refiner.

Simplified single groove model is used to analyze the flow in the rotor and stator of the refiner. Fluid is assumed to be Newtonian and single phase with dynamic viscosity 100 times higher than water. Model and mesh used for the rotor and stator are identical with different wall boundary conditions and fluid zone conditions. Simulations were performed with different pressure gradients and angular speed of the refiner.

The study shows that the flow in the rotor depends on the pressure difference and the speed of the refiner. Flow in the stator depends on the pressure difference; speed has little effect on the flow in the stator. In the rotor fluid flows towards the periphery while in the stator direction of flow is towards origin. Rotational motion is observed both in the rotor and the stator groove. This rotational motion carries the fluid into the gap, fibres present in the fluid form flocs and got stapled at the bar edge. They get treated every time a rotating bar crosses a stationary bar. To study the intensity of refining, strain rate and shear force is determined. Shear force is due to the rotation of the rotor and due to the motion of the fluid down into the groove along its wall i.e. fluid that is carried along with the rotating plate.

1 Table of content

LIST OF FIGURES

LIST OF TABLES

Chapter 1

1.1 Introduction

Pulp processing is an important phase in the paper production, it is being done through mechanical and chemical treatments and at times both processes are used in tandem to achieve the desired pulp properties. Mechanical pulping is the method of converting wood into cellulose fibres. Pulp yield (percentage of wood that become pulp) from mechanical process is between 80 to 95% whereas in chemical pulping yield is much less. Mechanical pulp provides high bulk and good opacity. In chemical pulping wood is treated in the presence of chemical and lignin in the wood is dissolved to create pulp. Chemical pulp creates higher sheet strength. The key difference between mechanical and chemical pulping is that the former does not destroy the lignin [1] [3]. The traditional method of mechanical pulping is by grinding stone in which wood logs are forced into the rotating stone, the surface of the stones is cut with patterns and through abrasive action of rotating stones wood is grounded to fibres.

Thermomechanical pulping (TMP) is a type of mechanical pulping, it is normally done at high consistencies; it has to large extent replaced the traditional methods of mechanical pulping. It is used in the production of paperboard, tissue, printing and writing papers. In this process wood is pre heated with steam and then it is treated inside the refiner under high temperature and pressure where fibres are mechanically separated. It is used to produce mechanical pulps and is usually done at 30-40 consistency.

Low consistency refining is also being used. It is mainly applied to the chemical pulps. It is considered more energy efficient as compare to the high consistency refining. Some people have studied its application to mechanical pulps as well [19]

The heart of Thermomechanical pulping is the Refiner, a hydraulic machine that can be thought of a less efficient pump, consisting of a set of rotating and stationary discs with multiple grooves, arranged in an array of generally radially extending grooves. The fibre suspension is pumped through the refiner and the fibres properties are improved as it passes through the set of bars and grooves. The process determines the quality of the finished product. Although different refiner designs are being used in industry, the

underlying principle is the same in all of them i.e. wood chips are fed into the machine consisting of at least two discs and one of them is rotating.

Although a lot of experimental studies have been carried out on the working of disc refiner, still there exist many ambiguities regarding the flow pattern inside the industrial refiner. The present study is an effort to understand the flow pattern inside the refiner and to numerically simulate the flow in the rotating and stationary part of the low consistency disc refiner. The purpose is to have an insight into how the fibre suspension moves inside the groove of the rotor and stator as well as in the small gap between the rotor and stator.

1.2 Problem definition

Refiner manufacturers and paper industry put large investments in the development and improvement of refining techniques. There are many areas within refining that are being explored. One important field is the energy consumption in the refiner and to develop ways that can produce energy efficient refining. In order to achieve that it is of utmost importance to understand the complex flow phenomenon inside the refiner and to identify the parameter necessary for the optimization of refining techniques and to enhance the efficiency of refining procedure.

The current study is the continuation of previous work performed by Magnus Björkman [16] under the supervision of Innventia and KTH. In previous study a refiner model was developed and flow pattern in the stationary part of the refiner was studied. In this work, the focus is on the flow in the rotating part of the refiner and its interaction with the stationary part. The aim of the study was to find an answer to the following questions.

- Study and analyze the development of the flow pattern inside the rotating and stationary part of refiner.
- Factors affecting the fluid flow inside the refiner.
- Effect of the fluid motion on the refining of fibres.
- Validation of experimental results carried out at Innventia.

In order to manage the complexity involved in this problem following limits were defined.

- A simplified model of refiner i.e. bars and groove model was used for the fluid flow analysis.

- A Newtonian fluid with constant viscosity was analyzed.

- A single phase fluid model is used.

- Fixed gap distance (the gap is the distance between the rotor and stator discs, this disc gap can be adjusted in industrial refiner)

- Heat generated during refining process is not considered.

2 Refining & refiners

Refining or beating plays a critical role in papermaking process. It's a process in which wood chips are mechanically treated to produce fibres and at the same fibre structure is changed to enhance its mechanical properties. Pulp properties such as absorbency, porosity and bonding ability of fibres are also improved. Unfortunately with the current refining techniques, alongside the desired structural changes few unsought changes in the fibre structure also take place, such as damage to pulp fibre. Thus mechanical refining is compromise between desirable and undesired changes in fibre properties. In an ideal mechanical pulping process the following phenomena are expected: fibres must be separated from the wood matrix, fibre length must be retained, fibres must be delaminated, abundant fines must be generated by peeling off outer layers of the middle lamella, primary and secondary layers of fibre wall, and finally the surface of the remaining secondary wall must be fibrillated [3] [4].

2.1 Effect of refining

Refining determines the quality and characteristic of the final product. Its aim is to effectively alter the fibre properties that eventually should lead to the improve product quality.

2.1.1 Fibre structural changes

Some of the major structural changes due to refining are listed down [6]

1. Cutting or shortening of fibre.

2. Fibre curling or removal of the curl.

3. External fibrillation.

4. Swelling or Internal fibrillation.

5. Fines production

2.1.2 Mechanical properties of fibres

Changes in the fibre structure have direct effect on the fibre's mechanical properties. Some major property changes are mention below.

1. Increase in tensile strength, tensile stiffness and internal bonding strength.

2. Tearing strength reaches a maximum during refining and thereafter decreases. [8]

3. Refining increases the fibre flexibility.

4. Refining decreases the Opacity of chemical pulp for mechanical pulp opacity increases [7]
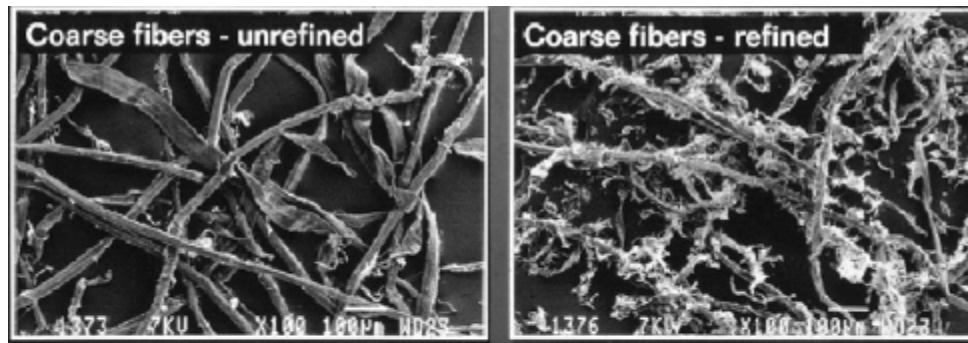
Figure 1: *Coarse fibre-unrefined (left) and refined (right) [7]*
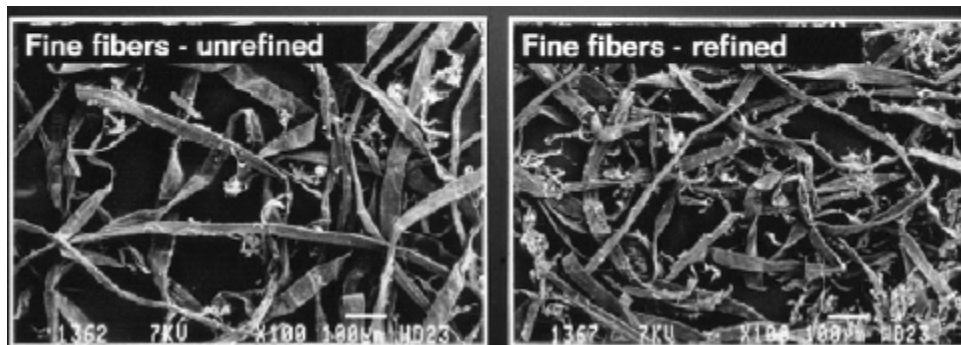
Figure 2: *Fine fibre unrefined (left) and fine fibre after refining (right) [7]*

2.2 The flow inside a refiner

A disc refiner can be compared with a radial centrifugal pump. The suspension or fluid is fed axially into the refiner at the centre of the disc. The rotating motion of the rotor plate imparts energy to the fluid and under the action of centrifugal force the fluid moves outwards in the radial direction. This rotating motion of the rotor changes the circumferential speed of the fluid and as a result a swirling motion of the fluid is created inside the groove of the rotor. The groove of the rotor must be wide enough to allow the fibre to rotate in the groove. The vortex flow that develops in the groove carries the

fibres and fibre get stapled on the bars, once stapled; the fibre gets treated as the bars moves on top of each other [4]. This treatment of fibres is termed as refining. Refining mechanism is explained by Jorma Lumiainen [4] in the form of figures as shown in figure 4.
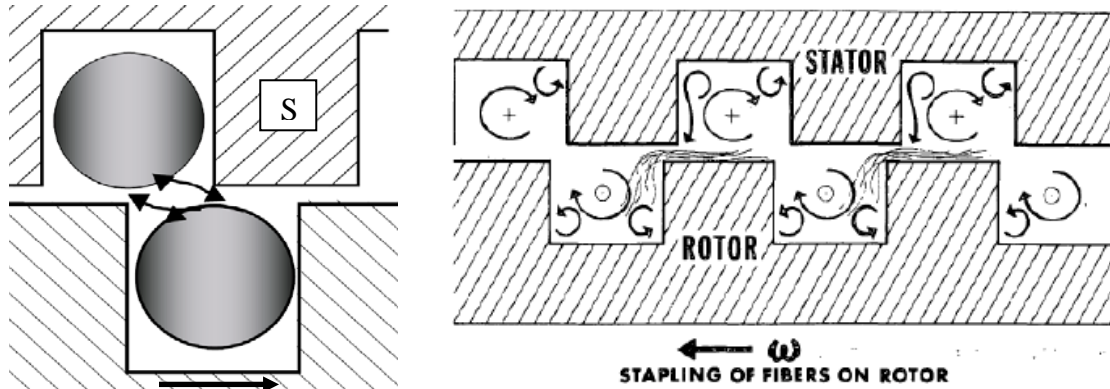
Figure 3:   *Rotational flow in grooves of refiner according to Lumiainen (Left) [4] & Fox (Right)[9].*

The outlet of the refiner is pressurized to regulate the flow leaving the refiner. Pressure at the outlet is higher than at the inlet. A part of the flow that do not leave the refiner enter into the stator and moves towards the center of the refiner due to pressure difference existing between the outlet and the inlet. This is necessary for the refining as the aim is to re-circulate the fluid a number of times before leaving the refiner to ensure that the fibres get treated in the gap region.

Fibre Pick up   Edge to edge fibre treatment   Edge to surface fibre treatment

| Surface to surface fibre treatment | Surface to surface fibre treatment | End of refining |
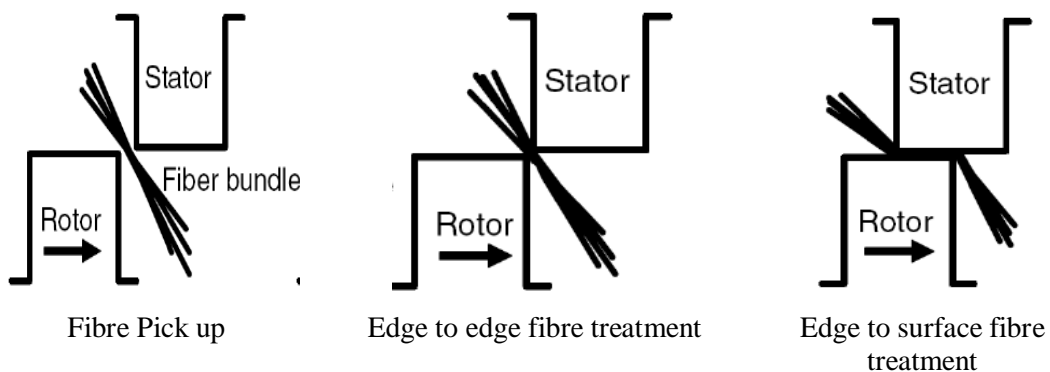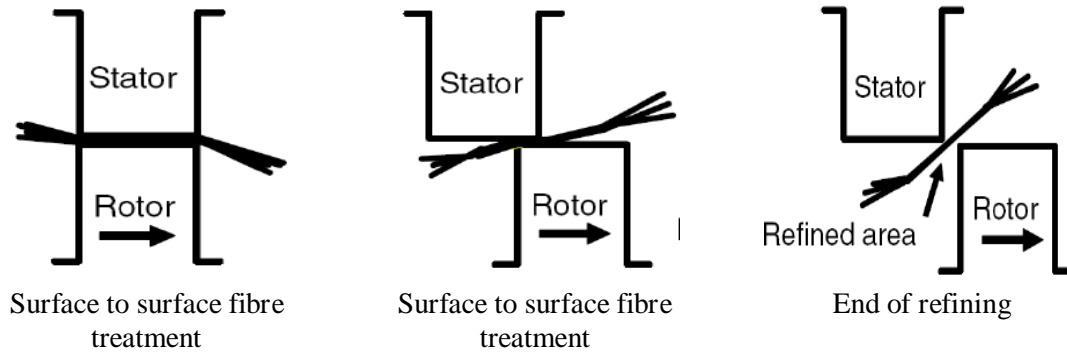
Figure 4: *Refining Mechanism*

The above sequence of step is repeated a number of times inside the refiner and fibre get refined in every step.

2.3 Refiners

There are two major refiner designs that are widely used in the industry with slight variation in plate designs, bar angles and plate arrangement;

1. Conical Refiners.   2. Disc Refiner

Various configurations of the refiners are shown in figure 5.

2.3.1 Conical refiner

Conical refiners have a conical rotor and it rotates inside a conical stator see figure 5. The fluid is pumped into the smaller end of the cone and is squeezed between the rotating and stationary cone.. In conical refiners the gap between stator and rotor can be controlled very accurately by adjusting the axial position of the rotor

2.3.2 Disc refiner

A disk refiner consists of two vertical disks with serrated or contoured surfaces. One disk rotates, while the other either remains stationary or rotates in opposite direction to that of the first disc. Fluid enters the machine axially, i.e. at the centre of the disc and the rotating disc imparts energy to the fluid causing it to move out of the machine in the radial direction at a relatively higher pressure. As the fluid is pushed outwards due to the rotating disc, the fluid get compressed in the narrow gap between the rotor and the stator. The abrasion experienced by the fibres during this process cuts, softens, rubs, and

disperses the fibres to the desired degree. The gap between the disks can be widened or shortened, depending on the extent of the refining appropriate to the end-use of the paper to be produced. Disc refiners are widely used in the paper making industry because of their simplicity of design and better performance compared to conical refiners.

The refiner studied in this work is a disc refiner that is being used at Innventia. It's a double disc refiner with a rotating plate in the middle of two stationary plates. The rotating and stationary plates have the similar bar and groove pattern. Bars and grooves are oriented at a certain angle.
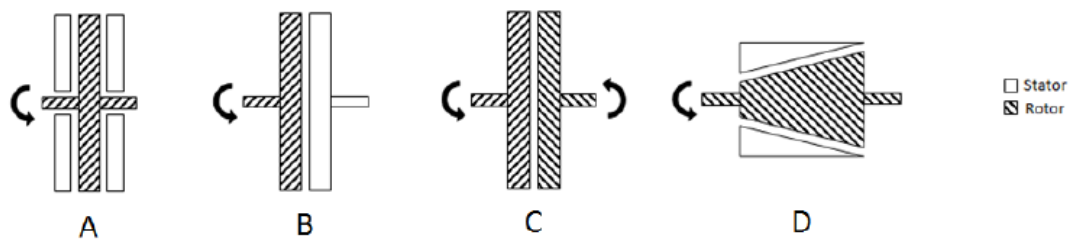
Figure 5:   *Various Refiner configurations [16]*

A: A Stator in the middle and two rotating plates on either sides of stator plate. Refiner at Innventia is of this type

B: A single rotor and Stator.

C: Two counter rotating plates.

D: A conical refiner.

3 Computational fluid dynamics

Computational fluid dynamics (CFD) has become vital in the analysis of problems involving fluid flows. Its technological value is undisputed and has become indispensable for design optimization. With CFD a large number of flow conditions can be simulated numerically at a considerably less cost and in relatively less time as compare to performing physical experiment. The idea is to divide the computational domain into smaller cells (or control volumes) comprising of nodes, and thereafter solving the problem using right boundary conditions. The solution to a flow problem (velocity, pressure etc) is defined at the nodes inside each cell.

3.1 Governing equations

The dynamics of a fluid is governed by the conservation laws of classical physics and the governing equations of the fluid flow are the mathematical form of these conservation laws, namely

- Conservation of mass, i.e. Continuity equation.
- Momentum conservation, i.e. the time rate of change of momentum of a body equals the net force exerted on it.
- Conservation of energy, i.e. rate of change of energy of the fluid is equal to the sum of rate of heat added to the fluid and the rate of work done on the fluid inside the control volume.

The formulations of these laws are under the assumption of the continuum hypothesis. In continuum hypothesis behavior of the fluid particle is described in terms of macroscopic properties such as velocity, pressure, density, temperature and their space and time derivatives and the molecular motion of fluid particle is ignored. It is valid when the size of the flow system is much larger than the mean free path between the molecules [18]. The momentum equation for viscous flow is identified as the Navier Stokes equation; however in broader terms it includes the entire system of equations governing the motion of fluid-continuity, momentum and energy. The flow in a disc refiner is incompressible. Furthermore in the present study the effect of temperature has not been considered, so the energy equation can be ignored. For incompressible, viscous flow inside the refiner the equations can be written as follows.

$$\frac{\partial u_i}{\partial x_i} = 0 \ \ (\mathbf{1})$$

$$\frac{\rho \partial u_i}{\partial t} + \rho u_j \frac{\partial u_i}{\partial x_j} = -\frac{\partial p}{\partial x_i} + \mu \frac{\partial^2 u_i}{\partial x_j \partial x_j} \ \ (\mathbf{2})$$

Where ρ is the density, μ is dynamics viscosity, p is the pressure and u is the velocity of fluid particle. The two terms on the left side of equation 2 are the unsteady acceleration and convective acceleration, whereas the terms on the right hand side represents the pressure forces, viscous forces and any external forces, respectively.

3.2 Finite volume methods

There are various methods by which partial differential equations describing the fluid flow can be solved numerically i.e. Finite difference methods, Finite element, spectral methods and Finite volume methods. The main difference between the above mentioned methods is how the flow variable are approximated and discretized. In this study Ansys Inc. Fluent solver has been used for the flow analysis, a solver based on finite volume methods. In case of the finite volume method, the numerical algorithm consist of following steps.[10]

- The geometrical domain is sub-divided into control volumes; the governing equation of the fluid flow is integrated over all the control volume of solution domain.
- Discretize the integral formulation of conservation laws over each control volume (Gauss divergence theorem), converting the integral equation into a set of algebraic equation.
- Solving the resulting set of algebraic equations.

The general conservative form for the fluid flow equation for the variable φ is given by [10]

$$\frac{\partial \rho \varphi}{\partial t} + \nabla(\rho \varphi U) = \ \nabla.(\Gamma \nabla \varphi) + \ q_\varphi \ \ (\mathbf{3})$$

Where φ is the fluid property, Γ is the diffusion coefficient or diffusivity and q is the source or sink.

Integration of the transport equation over control volume give the following equation [10].

$$\int_{cv} \frac{\partial \rho\varphi}{\partial t} dV + \int_{CV} \nabla(\rho\varphi U) dV = \int_{CV} \nabla.(\Gamma\nabla\varphi) dV + \int_{CV} q_\varphi \, dV$$

Using Gauss divergence theorem

$$\int_{cv} \frac{\partial \rho\varphi}{\partial t} dV + \int_{S} (\rho\varphi U).n \, dS = \int_{S} (\Gamma\nabla\varphi).n \, dS + \int_{CV} q_\varphi \, dV$$

By integrating the above equation over time, the general integrated form of transport equation is obtained.

$$\int_{\Delta t} \frac{\partial}{\partial t}\left(\int_{cv} \frac{\partial \rho\varphi}{\partial t} dV\right) dt + \int_{\Delta t}\int_{S} (\rho\varphi U).n \, dS dt = \int_{\Delta t}\int_{S} (\Gamma\nabla\varphi).n \, dS.dt + \int_{\Delta t}\int_{cv} q_\varphi \, dV dt$$

Where n is the outward unit normal vector. The above equation is valid for time dependent flows, in case of steady state flow the equation will reduce to

$$\int_{S} (\rho\varphi U).n \, dS = \int_{S} (\Gamma\nabla\varphi).n \, dS + \int_{CV} q_\varphi \, dV$$

3.3 Turbulence modeling

Most of the flows occurring in nature are turbulent in nature, they are random, chaotic, three dimensional, highly diffusive, dissipative and are characterized by the presence of strong eddies. The ratio of inertial forces to viscous forces known as the Reynolds number is a dimensionless number that can be determine in order to identify the fluid as laminar or turbulent. High Reynolds number flows are turbulent and inertial forces are comparatively higher than the viscous forces.

Fluid dynamics of turbulent flow is characterized by the existence of several length scales; Kinetic energy (through production mechanism) enters the turbulence at the largest scale of motion. This energy is transferred (by inviscid process) to smaller and smaller scales until reaching the smallest scale at which the energy is dissipated by the viscous action (Richardson 1922). The energy dissipation at small scale is given by the Kolmogorov scale.[11]

The Reynold Average Navier Stoke's equations are often used to describe turbulent flows. RANS equations are the time averaged equations of the motion for fluid flow. The flow field is decomposed into average and fluctuating part as [12]

$$U_i = \bar{U}_i + u'_i$$

$$P_i = \bar{P}_i + P'_i$$

Introducing the above decomposition in Navier Stoke Equation given in Eq 2, we get

$$\frac{\partial u'_i}{\partial t} + \frac{\partial \bar{U}_i}{\partial t} + \frac{u'_j \partial \bar{U}_i}{\partial x_j} + \bar{U}_j \frac{\partial u'_i}{\partial x_j} + \bar{U}_j \frac{\partial \bar{U}_i}{\partial x_j} + u'_j \frac{\partial u'_i}{\partial x_j} = -\frac{1}{\rho}\frac{\partial P'}{\partial x_i} - \frac{1}{\rho}\frac{\partial \bar{P}}{\partial x_i} + \nu \nabla^2 u'_i + \nu \nabla^2 \bar{U}_i \quad (4)$$

By taking the ensemble average of equation 4, the RANS equationis obtained.

$$\frac{\partial \bar{U}_i}{\partial t} + \bar{U}_j \frac{\partial \bar{U}_i}{\partial x_j} = \frac{1}{\rho}\frac{\partial \bar{P}}{\partial x_i} + \nu \nabla^2 u'_i - \frac{\partial}{\partial x_j}\left(\overline{u'_i u'_j}\right) \quad (5)$$

$$\frac{\partial \bar{U}_i}{\partial x_i} = 0$$

In the above equation, term $\overline{u'_i u'_j}$ is known as the Reynolds stress.

$$\overline{u'_i u'_j} = \begin{matrix} \overline{u^2} & \overline{uv} & \overline{uw} \\ \overline{uv} & \overline{v^2} & \overline{vw} \\ \overline{uw} & \overline{vw} & \overline{w^2} \end{matrix}$$

Thus from the RANS equation, results in 6 more unknown from the Reynolds stress tensor. In order to solve this system of equation various models have been proposed and are being used in numerical calculations. Some of them are;

- Zero Equation models.
- One equation models (Spalart-Allmaras Model)
- Two Equation Models. (k-ε model, k-ω model, k-ω SST model)

Two equation models are the most widely used turbulence model, most of these models solve a transport equation for turbulence kinetic energy and a second transport equation allowing the turbulent length scale to be defined. The most common among these is the k-ε (Launder & Spalding 1974) model in which the second equation is the turbulent dissipation. Transport equations for standard eddy viscosity k-ε model are [13]

$$\frac{DK}{Dt} = P_k - \varepsilon + \frac{\partial}{\partial x_k}\left[\left(\nu + \frac{\nu_T}{\sigma_K}\right)\frac{\partial K}{\partial x_k}\right] \quad (6)$$

$$\frac{D\varepsilon}{Dt} = (C_{\varepsilon 1}P_k - C_{\varepsilon 2}\,\varepsilon)\frac{\varepsilon}{K} + \frac{\partial}{\partial x_k}\left[\left(v + \frac{v_T}{\sigma_\varepsilon}\right)\frac{\partial \varepsilon}{\partial x_k}\right] \quad (7)$$

$$P_k = 2v_T S_{ij} S_{ji}$$

$$v_T = C_\mu \frac{K^2}{\varepsilon}$$

Model Coefficients standard values are

$$C_\mu = 0.09 \quad C_{\varepsilon 1} = 1.44 \quad C_{\varepsilon 2} = 1.92 \quad \sigma_K = 1.0 \quad \sigma_\varepsilon = 1.3$$

In equation 6 & 7 P_K denotes production of turbulent kinetic energy.

Large eddy simulation (LES) is another method used for modeling of turbulent flows. It solves the larger scales of turbulence directly while modeling the smaller scales. Because it solves the larger scales explicitly, LES provides more accurate results, than the RANS models. On the other hand LES requires a finer mesh and is more computationally expensive.

3.4 Moving reference frame

A moving reference frame or non inertial frame of reference is fixed with respect to an inertial or stationary frame of reference. A system rotating with certain angular velocity relative to a stationary frame can be represented as
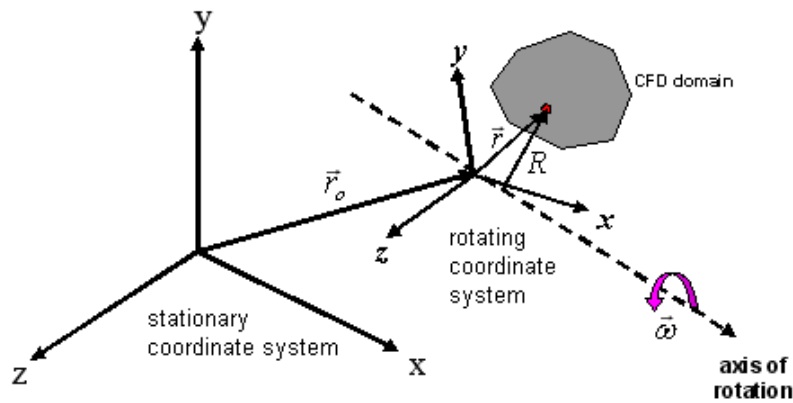
Figure 6:   *Stationary and moving reference frame* [14]

Problems involving rotational motion can be modeled using a non inertial frame of reference. Equations of motions describing a moving reference frame (non inertial) includes the effect of coriollis and centrifugal forces.

Fluid velocities can be transformed from the stationary frame to the rotating frame using simple relations [14]

$$V_r = v - u_r$$

Where

$$U_r = \Omega * r$$

Where V_r is the relative velocity, v is the absolute velocity and U_r is the velocity of moving frame with reference to relative frame.

Using above transformation it is possible to write the Navier stoke equation in terms of relative velocity formulation or in terms of Absolute velocity formulation [14]

$$\frac{\partial v_r}{\partial t} + v_r.\nabla v_r = -\frac{1}{\rho}\nabla p + g + \nu\nabla^2 v_r - (2\Omega \times v_r) - (\Omega \times \Omega \times r) \quad (8)$$

$$\nabla. v_r = 0$$

Equation 8 gives the relative formulation of Navier stoke equation for rotating reference frame. In this equation $-(2\Omega \times v_r)$ gives the coriolis force and $(\Omega \times \Omega \times r)$ is the centrifugal force [14].

With the absolute velocity formulation the momentum equation is

$$\frac{\partial v}{\partial t} + v .\nabla v = -\frac{1}{\rho}\nabla p + g + \nu \nabla^2 v - (\Omega \times v) \quad (9)$$

In Equation 9, coriollis and centrifugal force collapsed into single form $(\Omega \times v)$.

4 Models and geometrical setup

4.1 Model[1]

The disc refiner consists of a circular plate, which is made up of number of sectors. Each sector consists of multiple grooves (figure 7B). In this study a simplified model is considered for the flow analysis in the rotor and in the stator of the refiner. The simplified single groove model is shown in figure 7C. In a disc refiner there are two circular plates, the second plate is represented by the flat plate in the single groove model.
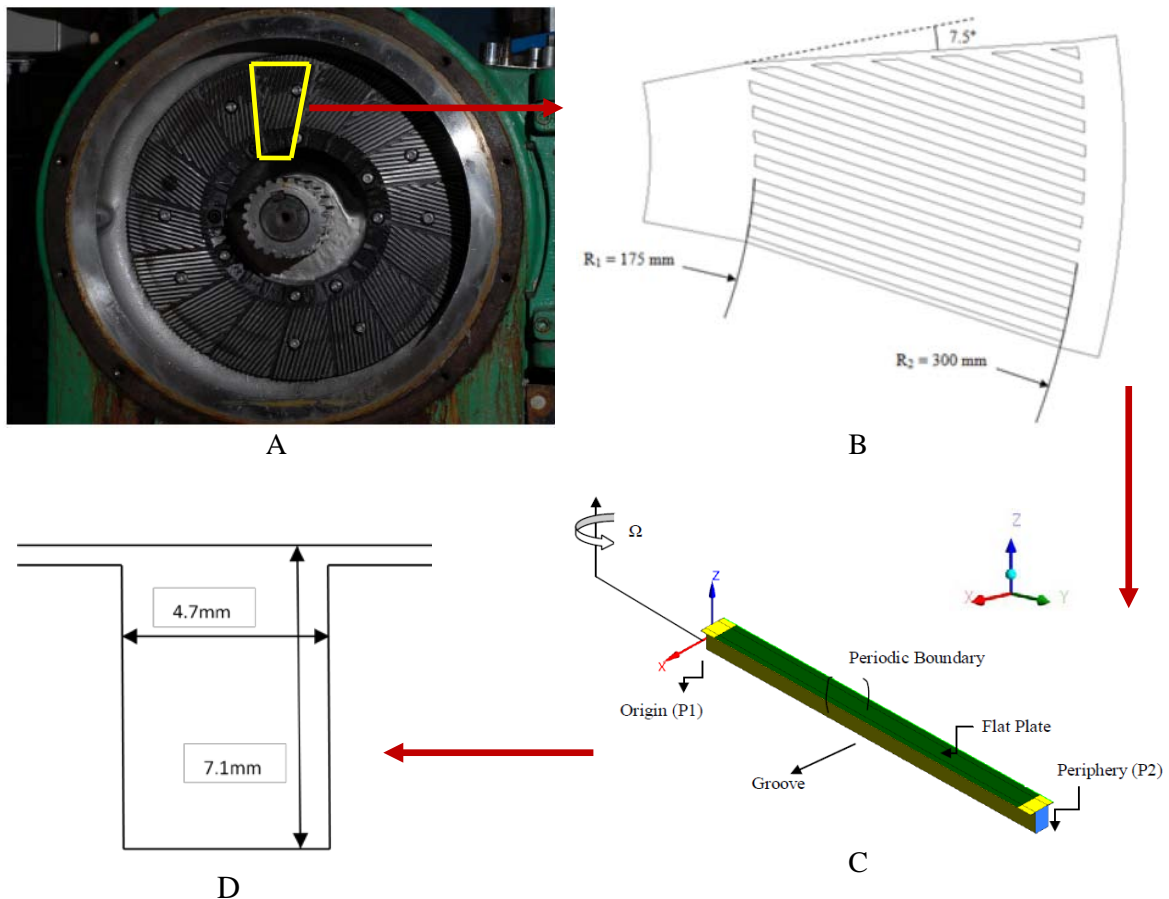
A: Original Disc Refiner plate with multiple sectors, B: Sector consisting of multiple grooves, C: Model for single groove with flat plate, D: Cross section of single groove model.

Figure 7:   *Model Detail*

---

[1] Model created by Magnus Björkman, MS Thesis 'Numerical Modeling of flow in Refiner'

Origin of the single groove model is located at 175mm from the centre of the refiner. Length of the groove model is 125mm. It is rotating around z axis and motion of the fluid is along y-direction.

Figure 8 shows the difference between the actual and simplified case. Flow in the rotor and stator were separately analyzed.

Rotor

Actual Case

Rotor

Simplified case-Flow in the rotor groove

Rotor

Simplified case-Flow in the stator groove
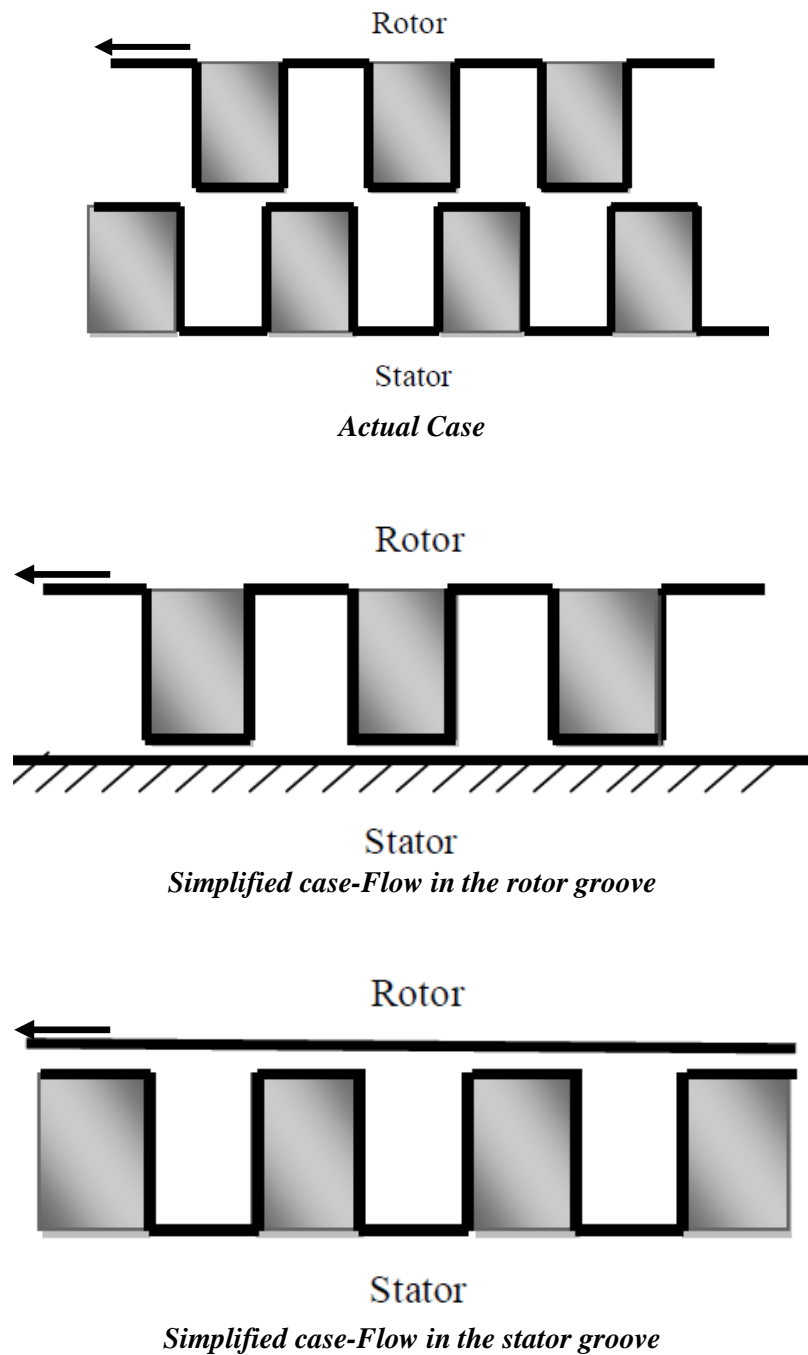
Figure 8:   *Difference between the actual case and the simplified model*

In the current study the flow inside the rotor is modeled using the moving reference frame with the rotational periodic boundary condition. The flow inside the stator was modeled using the stationary reference frame with the rotational periodic boundary condition. Rotational periodic boundary condition is applied on the rotating flat plate because of its cyclic symmetry. In the rotor model the groove represents the rotor and the flat plate represents the stator. In the stator model the groove represent the stator and the flat plate represent the rotor. Due to rotational motion of the model i.e. angular speed, linear velocity increases continuously in the radial direction($V = rw$).

4.1.1 Model for the rotor

In rotating model it is important to keep track of reference frame, one way to visualize the model is in absolute frame of reference as seen by the stationary observer looking from outside the refiner, in such a case groove will appear rotating to the stationary observer and flat plate will appear stationary as shown in figure 9. The colour code represents the velocity distribution due to the rotational motion.
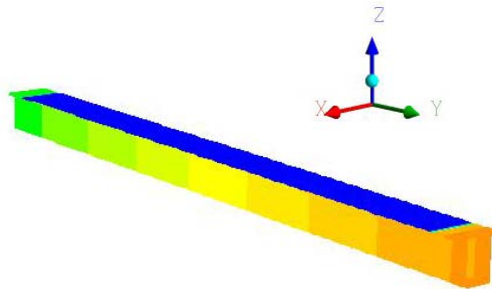
Figure 9:   *Rotor Model (Absolute frame of reference)*

Another approach is to visualize the problem in a relative reference frame; In this case it can be assumed that observer is inside the refiner groove and is rotating with the groove than to such an observer flat plate will appear moving in the direction opposite to the direction of rotation of groove as shown in figure 10.

As mentioned before that in the rotor model flat plate represents the stator, but in this report rotor results are presented in relative frame of reference due to this flat plate is always considered as rotating.
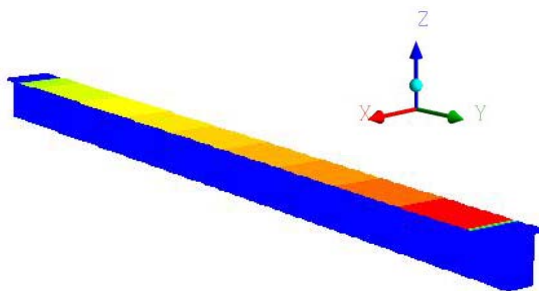
Figure 10:   *Rotor Model (Relative frame of reference)*

4.1.2 Model for the stator

In the stator model stationary reference frame is used. Flat plate represents the rotor and is rotating with certain angular speed. Groove is considered as stationary and it represents the stator.
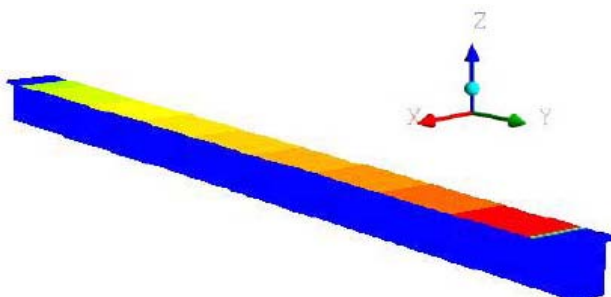
Figure 11:   *Stator Model (Stationary reference frame)*

4.2 Mesh

The mesh used in the simulation was created using ANSYS ICEM CFD, since the geometry of the model is made up of plane and orthogonal plane surfaces a mapped mesh with hexahedral elements was used. The mesh used in this study consists of 284031 elements. Mesh for the groove model is shown in the figure 11
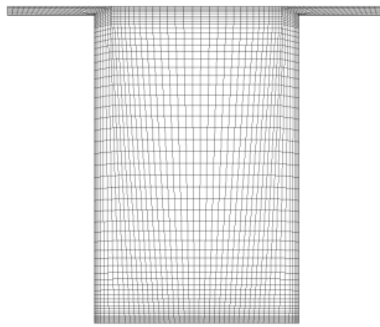
Figure 12: *Mesh for the model[2]*

4.3 Computational set up

In this study fluid is considered as incompressible, single phase and Newtonian. Simulations were performed for a fluid with viscosity 100 times that of water (0.1Pa-s). Viscosity of 0.1Pa-s was selected on the basis of results obtained in the previous study [18]. Results with fluid viscosity of 0.1Pa-s were found similar experimentally obtained results at Innventia.

4.3.1 Turbulence modeling

k-ε turbulence model is used in this model. At the origin along with pressure boundary condition a turbulent intensity of $1 \frac{m^2}{s^2}$ and turbulent dissipation rate of $1 \frac{m^2}{s^3}$ is specified. At the periphery, backflow turbulent intensity of $1 \frac{m^2}{s^2}$ and backflow turbulent dissipation rate of $1 \frac{m^2}{s^3}$ is specified.

The turbulence intensity of 1% or less is generally considered low, in this model with the viscosity of 0.1Pa-s, turbulence intensity is considerably less at the low refiner speed, and it increases slightly with the increase in refiner.

4.4 Boundary conditions

Pressure boundary conditions are used at the origin and the periphery of the model. The flat plate is considered as a rotating wall with the rotational periodic boundary conditions. Rotational motion is defined in terms of angular speed as shown in table 1. At the surface of the wall no slip boundary condition is used, it means the velocity of the fluid particle at the surface is zero.

---

[2] Mesh created by Magnus Björkman using ANSYS IcemCFD.

4.4.1 Pressure boundary conditions

Pressure boundary conditions are used at the origin and periphery of the model (see figure 7). Pressure values used are the pressure difference measured at the inlet and outlet of the Disc refiner at Innventia.

As the pressure values at the origin and the periphery of the groove model are not known, it is important for the modeling of a single groove to determine the right pressure difference and the corresponding refiner speed. In order to find that a number of simulations were performed with different pressure differences and refiner speed, and the results were compared with the experimental results from Innventia and with the results reported in reviewed literature.

To begin with a tentative value of pressure difference at which centrifugal forces and radial pressure forces are in equilibrium can be determined by considering the relation given below, this relation do not consider any losses, so the actual values would be higher than the values obtained from this relation.

$$\frac{\partial P}{\partial r} = \rho \Omega^2 r$$

The radial pressure gradient at which centrifugal forces are in equilibrium is given in Table 1.

RPM	Angular speed (rad/s)	ΔP (kPa)
600	63	117
750	78	180
900	94	262

Table 1: *Equilibrium between pressure difference and centrifugal force*

4.4.2 Periodic boundary condition

The refiner disc consist of multiple bar and groove patterns, due to this periodically repeating nature of the geometry it is possible to use the rotational periodic boundary condition with no pressure drop. Rotational periodic boundary conditions are defined at the two side surfaces as shown in figure 7.

4.4.3 Summary of Model

Fluid Model	Incompressible, Newtonian
Fluid Density	998 Kg/m^3
Fluid Viscosity	0.1 Pa-s
Turbulence Model	k-ε Turbulence model
Reference Frame	Stationary & Moving Reference Frame
RPM	600, 750, 900
Boundary Conditions	
Origin	Pressure Inlet
Periphery	Pressure Outlet
Periodic	Rotational
Wall	No Slip condition at Wall
Wall Motion	In Rotor model groove wall is defined as rotor, whereas in stator model flat plate is defined as rotating wall

Table 2:   *Material properties and boundary conditions used in the simulation.*

5 Results

Based on the boundary conditions mentioned in section 4.3, the model for the rotor and the stator was solved using Fluent. It was found out that the flow inside the refiner depends on the pressure difference between the origin and the periphery of the groove, and on the angular speed of the flat plate. Forces that drives the fluid in the rotor is the centrifugal force, generated by the rotational motion of the rotor and pressure difference acts as a resistive force to the fluid motion. In the stator fluid flow is only due to pressure difference.

In this section effects of pressure and speed on the mass flow rate through the rotor and the stator and on the flow velocity components in the groove of the rotor and the stator are analyzed.

5.1 Mass flow rate through refiner

According to Fox [9] and experimental results obtained at Innventia, the mass flow rate in the rotor has to be higher than the mass flow rate in the stator of the refiner. Table 3 indicates the mass flow rate through the rotor and the stator at different pressure differences and refiner speed. On the basis of table 3 it is possible to determine the pressure differences and the corresponding speeds that give the mass flow rate as observed in the experiments. Highlighted cases are the ones in which absolute mass flow rate is higher in the stator, which is not the desired condition and hence can be neglected.

	RPM	ΔP=50 kPa	ΔP=75 kPa	ΔP=100 kPa	ΔP=125 kPa
R	600	0.098	0.058	0.011	-0.035
S	600	-0.087	-0.124	-0.157	-0.188
R	750	0.171	0.140	0.106	0.067
S	750	-0.086	-0.122	-0.154	-0.185
R	900	0.253	0.225	0.197	0.167
S	900	-0.085	-0.120	-0.152	-0.182

Table 3: *Mass flow rate (kg/s) in the rotor and stator groove at different pressure gradients and RPM, R= Rotor, S=Stator*

5.1.1 Variation of mass flow rate with pressure and speed

The mass flow rate in the rotor depends on the speed of the rotor and on the pressure gradient. At higher pressure gradients more resistance is offered to centrifugal force as a result mass flow rate decreases with the increase in the pressure gradient at constant speed. It can be seen in the table 3 that at constant speed magnitude of mass flow rate in the rotor is decreasing with the increase in pressure gradient.

The negative sign of mass flow rate in the rotor at pressure difference of 125 kPa and 600 RPM shows that the fluid is not going towards the periphery. The fluid is moving towards the origin due to the weak centrifugal force so this case can be neglected as it does not depict the actual flow condition in the rotor of refiner. Similarly for the remaining highlighted cases in the table 3, the mass flow rate in the rotor is smaller in magnitude as compare to mass flow rate in the stator. Thus these conditions are ignored.

Mass flow rate in the stator does not depend upon the speed, but is affected with the change in the pressure gradient. It increases with the increase in pressure gradient. As there is no centrifugal force present in the stator, there is no resistance to the flow, therefore, the higher the pressure difference the higher the mass flow rate in the stator.
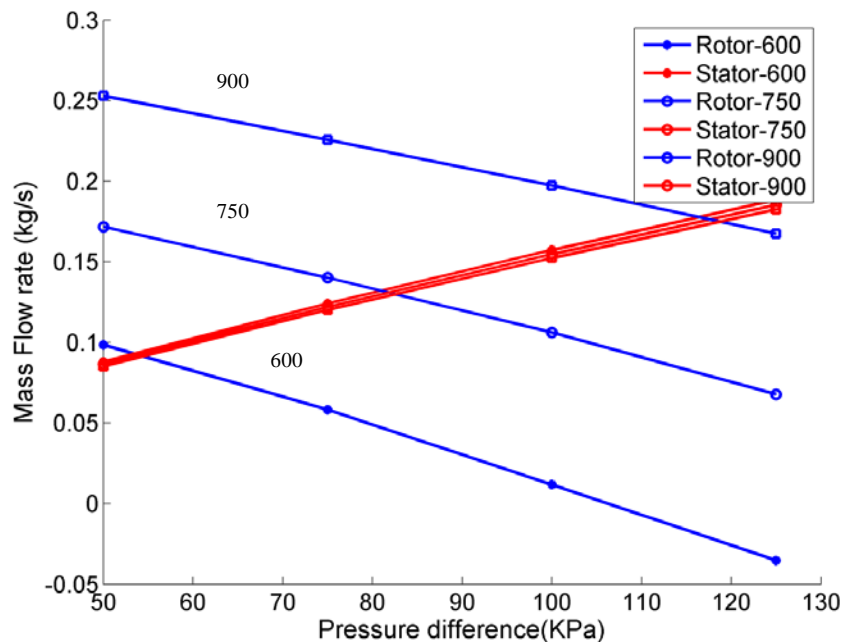
Figure 13: *Mass flow rate through rotor (blue) and stator (red) at different pressure gradient and RPM.*

Figure 13 shows the variation of mass flow rate through the rotor and the stator with the change in the refiner speed and the pressure difference across the groove. Blue lines represent the absolute mass flow in the rotor and the red lines indicate the absolute mass flow through the stator. In the rotor the magnitude of the mass flow rate decreases with the increase in pressure. This is due to the counteraction of the centrifugal force, whereas in the stator the mass flow rate increases with the increase in pressure.

At higher speed the mass flow through both rotor and stator increases, however speed has a negligible effect on the mass flow through the stator.

5.1.2 Net mass flow rate

The difference in mass flow rate through the rotor and the stator will give the net mass flow rate. Table 4 shows the net mass flow rate through a refiner. Cases with the negative mass flow rates can be neglected, as in these cases mass flow rate through the stator is higher than the rotor, which is not the desired condition.

Net Mass Flow Rate (kg/s)				
RPM	ΔP=50 kPa	ΔP=75 kPa	ΔP=100 kPa	ΔP=125 kPa
600	0.010	-0.065	-0.145	-0.153
750	0.085	0.018	-0.048	-0.117
900	0.168	0.105	0.044	-0.015

Table 4: *Net mass flow rate (kg/s)*
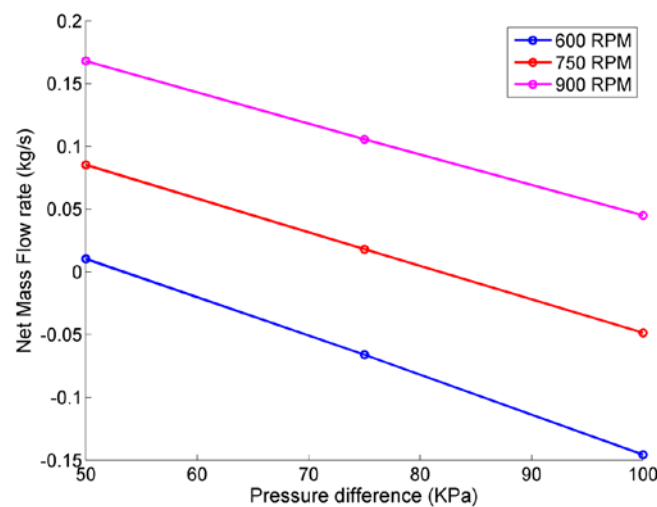
Figure 14: *Net Mass flow rate through refiner at different pressure difference and speed.*

Figure 14 shows that the net mass flow rate decreases with the increase in the pressure gradient and the overall mass flow rate increases with the increase in the refiner speed. For the same pressure gradient higher mass flow rate is obtained at higher speed.

5.1.3 Comparison of experimental data and CFD result

In order to validate the results from the numerical model, the results were compared with the experimental results obtained from Innventia. Figure 15, shows the results from the experimental study performed at Innventia. It shows the flow speed inside the stator groove. Numerical and experimental results for the stator follow the same trend, i.e. an increase in pressure difference increases the flow velocity or the mass flow rate along the groove.
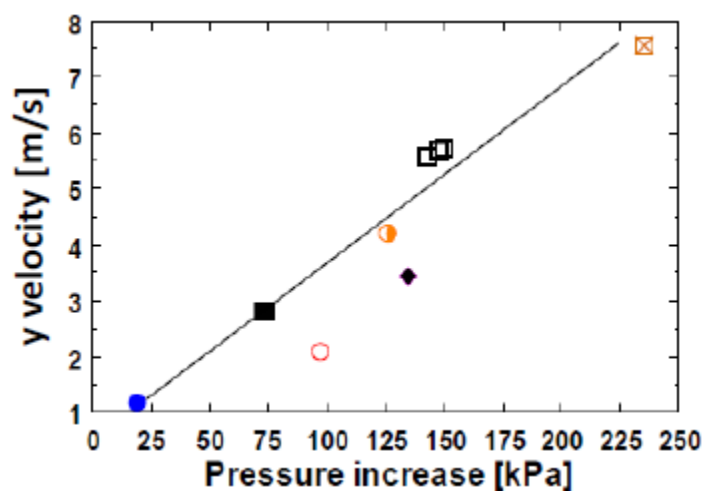
Figure 15:   *Flow through the stator groove at different pressure gradient (by Ulla-Brit Mohlin)*

5.2 Variation of flow velocity with pressure and speed

The pressure gradient affects the magnitude of the velocity components in the groove. Table 5 displays the volumetric average of velocity magnitude in the groove. Compared to the stator, the velocity in the rotor is high, a feature also observed by Fox [9]. The magnitude of velocity is affected by the change in the speed of the refiner and by changing the pressure difference between the origin and periphery.

Volume Average of Velocity Magnitude (m/s)					
	RPM	ΔP =50 kPa	ΔP =75 kPa	ΔP =100 kPa	ΔP =125 kPa
R	600	13.5	13.2	13.1	13.2
S	600	3.2	4.2	5.1	5.9
R	750	17.1	16.8	16.6	16.4
S	750	3.4	4.3	5.2	6.0
R	900	21.1	20.8	20.5	20.2
S	900	3.6	4.5	5.3	6.1

Table 5: *Flow velocity through stator and rotor at different pressure gradients and rotor speed.*

The velocity magnitude represents the sum of all the velocity components and in order to have a better picture of the flow condition inside the refiner it's better to analyze the individual velocity components.

The y-velocity (y-direction) is an indicator of transportation of fluid along the groove. In the case of the rotor, y-velocity decreases with the increase in pressure gradient at constant speed and in stator, the y-velocity increases as shown in table 6.

Volume Average of Y- Velocity(m/s)					
	RPM	ΔP =50 kPa	ΔP =75 kPa	ΔP =100 kPa	ΔP =125 kPa
R	600	2.80	1.7	0.3	-1.0
S	600	-2.5	-3.5	-4.5	-5.4
R	750	4.9	4.00	3.0	1.9
S	750	-2.5	-3.5	-4.4	-5.3
R	900	7.2	6.4	5.6	4.7
S	900	-2.4	-3.4	-4.3	-5.2

Table 6: *Y-Velocity through rotor and stator at different pressure gradients and rotor speeds.*

As shown in figure 7, the periphery is in positive y direction, so the fluid going towards the periphery is represented by a positive sign i.e. flow in the rotor is going towards the periphery. Negative sign indicates a direction towards the origin i.e. Stator.

Table 6 can be compared with the table 3. Highlighted cases are not considered. Based on the experimental studies, magnitude of flow velocity in radial direction (Y-direction) has to be higher in the rotor than in the stator.

5.2.1 Effect of pressure difference

Figure 15 shows the effect of the change in pressure gradient on the flow pattern in the groove of the rotor and the stator at constant refiner speed of 900 RPM. These are the velocity contour plots at the midplane (62.5mm) for pressure gradients of 50 kPa, 75kPa and 100kPa.

Flat plate is rotating in the positive x-direction. 900 RPM is selected because at this speed mass flow rate in rotor is greater than the stator. See Table 3
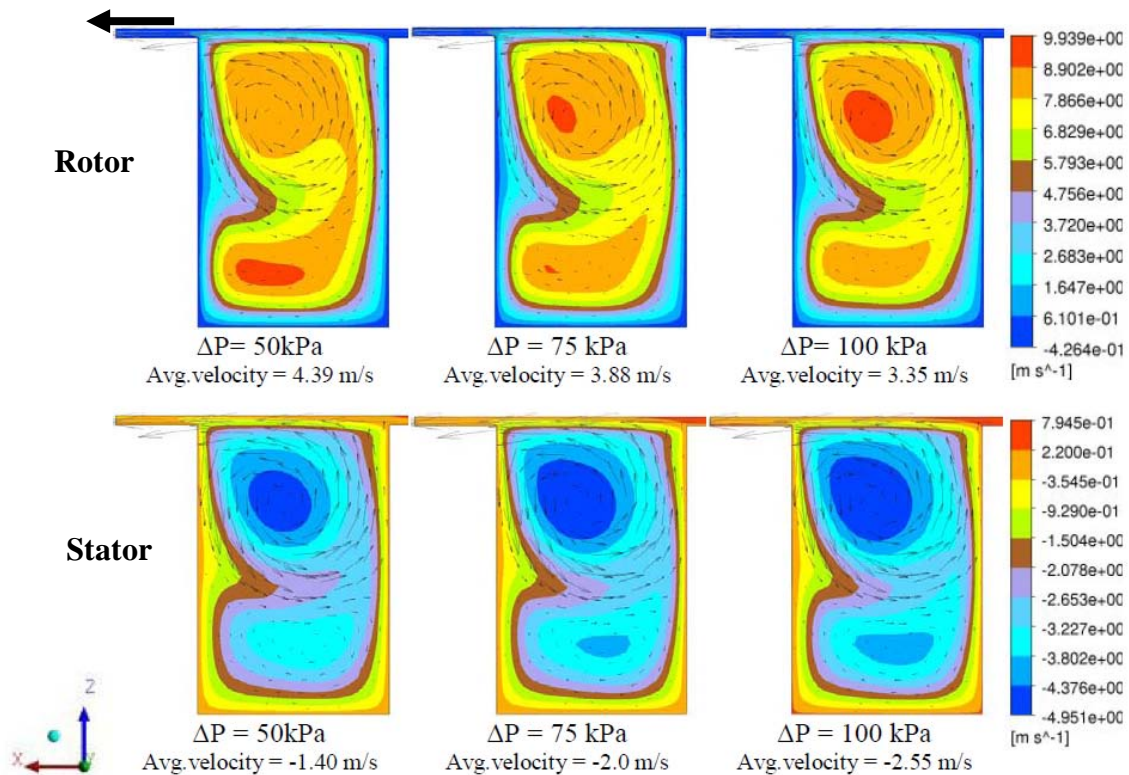
Figure 16: *Variation of Y-velocity with pressure difference, cross section located at midplane (62.5mm), rotor speed 900RPM.*

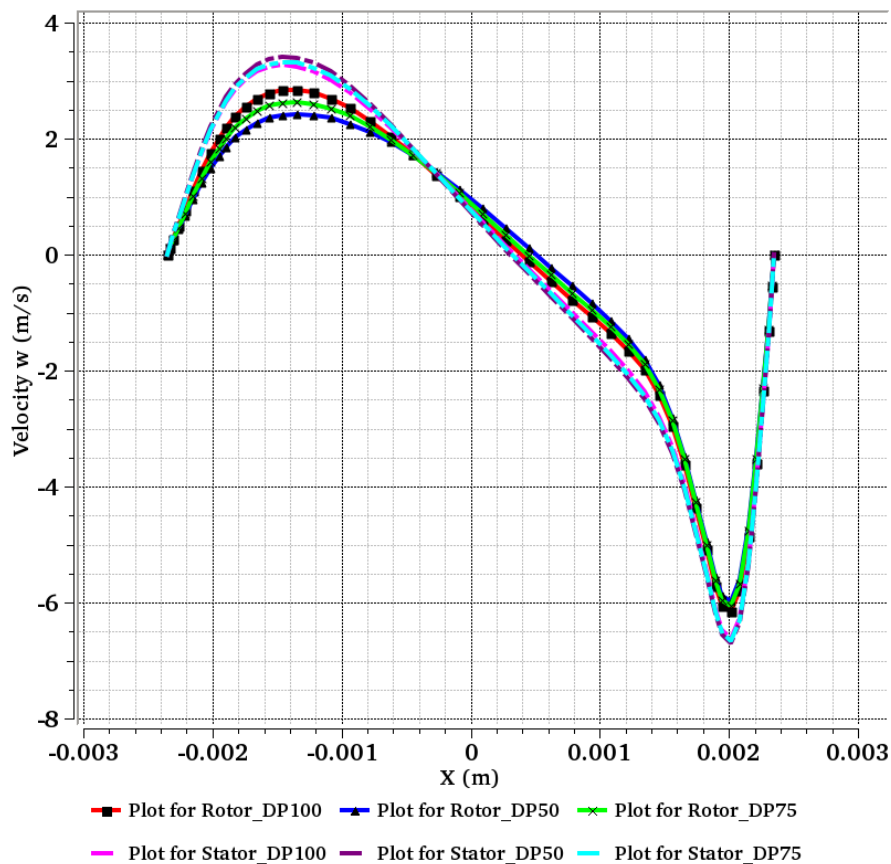Figure 16 shows y-velocity distribution in the refiner, y-velocity in the rotor is comparatively higher than in the stator.

Comparison of the flow pattern in the rotor at different pressure differences shows that for 50 kPa, the y-velocity is higher in the bottom of the groove, with the increase in the pressure difference, the y-velocity in the bottom of the groove decreases at the same cross section.

At the top of groove strength of y-velocity is less at 50 kPa and it increases with the increase in the pressure. The y-velocity tends to decrease in the bottom of rotor groove and increases in the top of the rotor groove as the fluid moves along the groove. This is due to shift of fluid stream from bottom to the top, see figure 24. It can be said that the increase in the pressure favours the upward motion of fluid particle in the rotor groove that ultimately leads to higher flow velocity at the top of the rotor groove. Average flow velocity decreases in the rotor with the increase in the pressure difference.

In the stator average radial velocity is comparatively less than the rotor. Rotational motion in top of stator groove is very high; increase in pressure increases the strength of rotational flow in top portion of stator groove.

Figure 17 show the distribution of z-velocity at a cross section located in the midplane (62.5mm). Rotational motion is due to this velocity component.

Figure 17:   *Z-Velocity distribution in rotor and stator groove at constant RPM and different pressure gradients. RPM =900, ΔP= 50, 75& 100 kPa.*

Rotational velocity changes slightly in both rotor and stator due to change in pressure; Graphical display gives a good picture of rotational flow in the refiner. It is slightly higher in the stator as depicted by the 3 dashed lines in figure 17. Magnitude of rotational velocity is very high in the direction of motion of flat plate i.e. positive x-direction.

5.2.2 Effect of refiner speed

The flow velocity increases with the increase in the refiner's speed; see Table 5 & 6. The y-velocity in Table 6, shows a very slight decrease in velocity with the increase in the speed, this is due to increased mass flow rate through rotor.

Increasing the speed of refiner changes the magnitude of flow velocity, but it does not have any significant impact on the flow pattern or velocity distribution in the groove. Figure 19 & 20, shows the distribution of x, y and z component of velocities at midplane in rotor and stator groove. It follows the same trend as explained in section 5.1.4, other than the fact that magnitude of velocity increases with the increase in speed.

In figure 19 & 20, x, y and z velocities are plotted in the middle of the groove. To compensate for the location of centre of rotation the data in figure 19 & 20 is sampled with 0.5mm offset in x-direction and for velocities in y and z directions it was sampled with 2mm offset in z-direction.
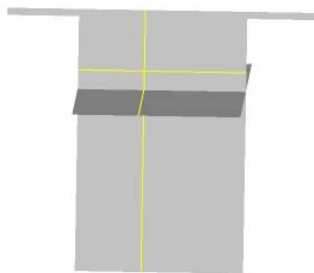
Figure 18:   *Lines used for data sampling x, y and z velocities*

The flow velocity along the rotor groove i.e. positive y-direction is significantly affected with the change in the refiner speed. Increasing the speed of the refiner will increase the flow velocity as shown in figure 18.

In the stator, y-velocity does not change with the increase in the refiner's speed. It stays almost constant throughout the groove. The only difference is that the fluid is going towards the origin i.e. negative y-direction, in the stator.
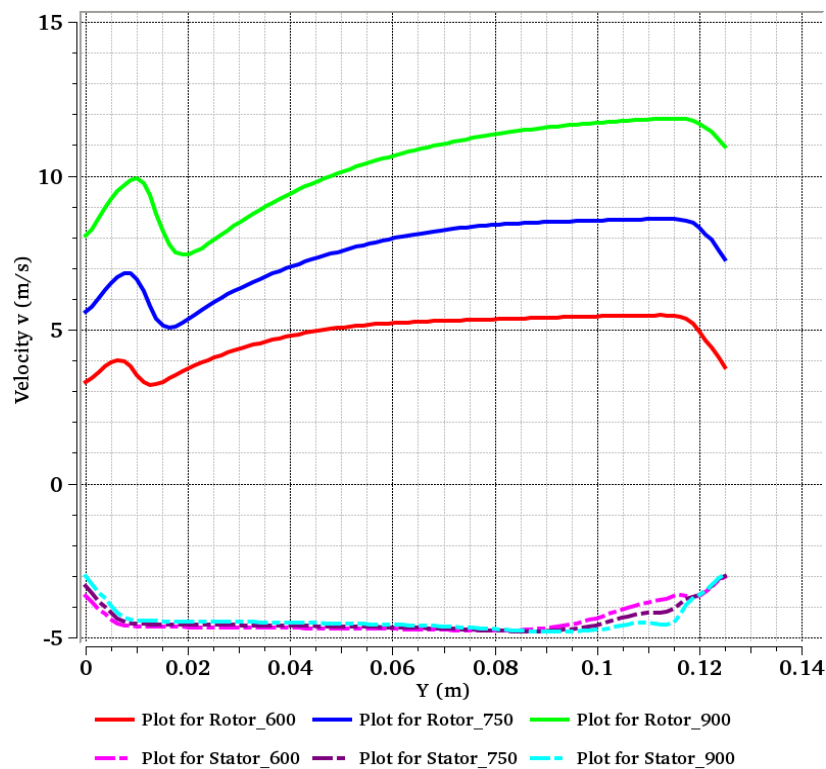
Figure 19: *Variation of Y-Velocity in the rotor and the stator with the change in refiner speed.*

Change in the refiner speed do not have any significant impact on the distribution of x and z velocity across the groove. Figure 20 shows the plot of z-velocity in the groove, it can be seen that z-velocity is slightly higher in the stator (dashed lines) as compare to the rotor.

X-velocity distribution is very similar in the rotor and in the stator. Inside the groove its variation due to the change in speed is small. Near the rotating flat plate, x-velocity is high for the higher refiner speed as shown in figure 20.
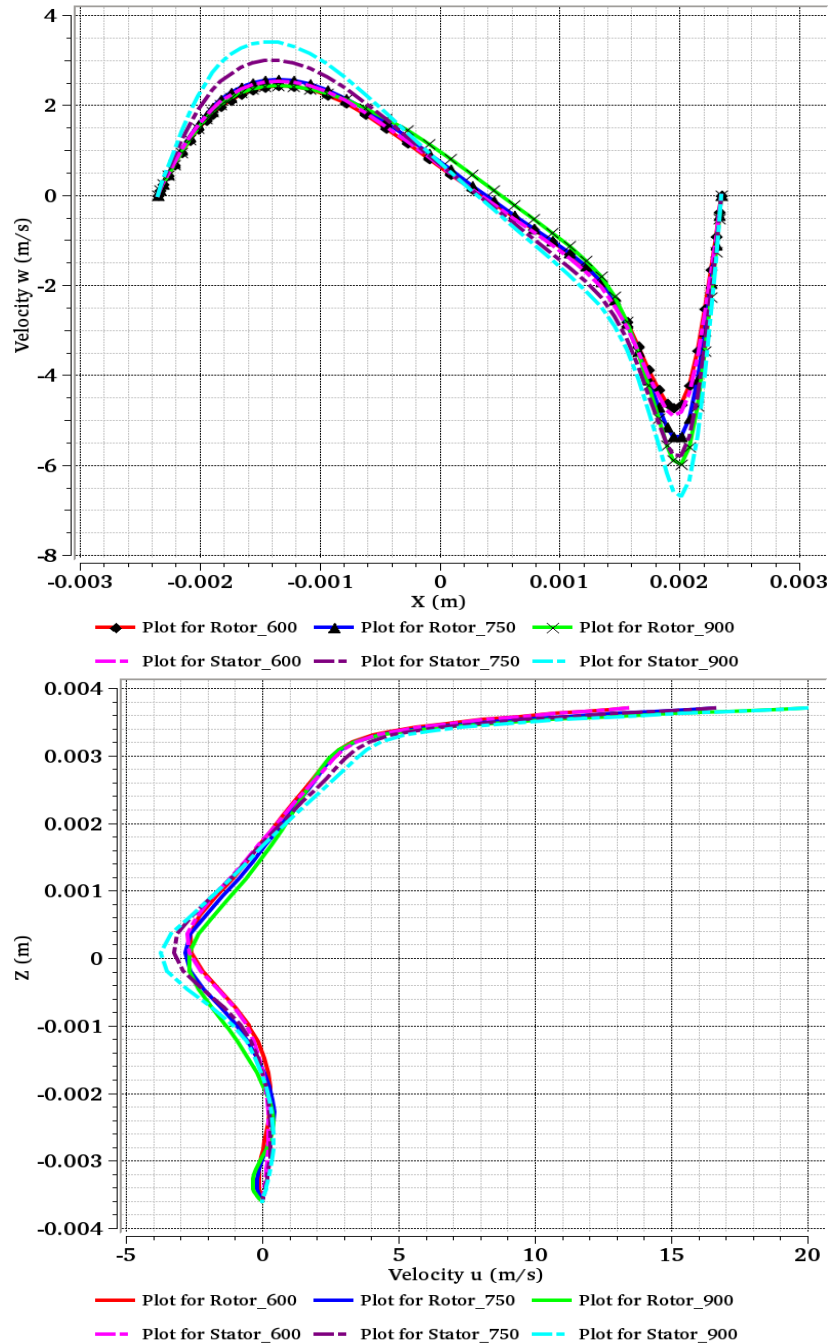
Figure 20: *Variation of Z (Top) & X-velocity (Bottom) with the change in refiner speed.*

5.3 Flow development in a refiner

Inside the refiner the main flow is along the grooves, transportation of fluid is in the groove of rotor. Backflow is observed in the groove of the stator. Flow in the gap is also very significant as most of the refining takes place in the gap. Flow in the rotor, stator

and in the gap are separately analyzed. Results presented below are for the rotor speed of 750 RPM and pressure difference of 50 KPa. Viscosity of the fluid is 0.1Pa-s.

5.3.1 Flow in the rotor

Flow in a rotor depends upon the pressure difference and speed of the refiner, in this section y and z-velocity along the groove at different cross section is analyzed

5.3.1.1 Y-velocity

The y-velocity represents the transportation of fluid along the groove. The y-velocity in general increases as the fluid moves along the groove. Distribution of y-velocity is not uniform due to complex flow conditions inside the groove. A closer look at figure 21 shows that at the start of the groove magnitude of y-velocity is very high in the bottom of the groove and is less at the top. This is due to the presence of the weak rotating or swirling motion at the top of the groove that is developed in the top part due to rotation of flat plate, as a result more fluid is being transported in the radial direction (Red region at 30mm and 45mm). As the fluids move ahead, swirling motion at the top gets stronger due to contribution of fluid from the bottom and also due to increase in the magnitude of centrifugal force.

Fluid in the bottom of the groove starts to shift upward; this motion of fluid streams from bottom to top adds energy to the rotational motion at the top, as a result radial velocity starts to increase in the top of the groove after the midplane see cross section at 75mm in figure 21. Near the exit magnitude of y-velocity becomes very strong in the top half of the groove.
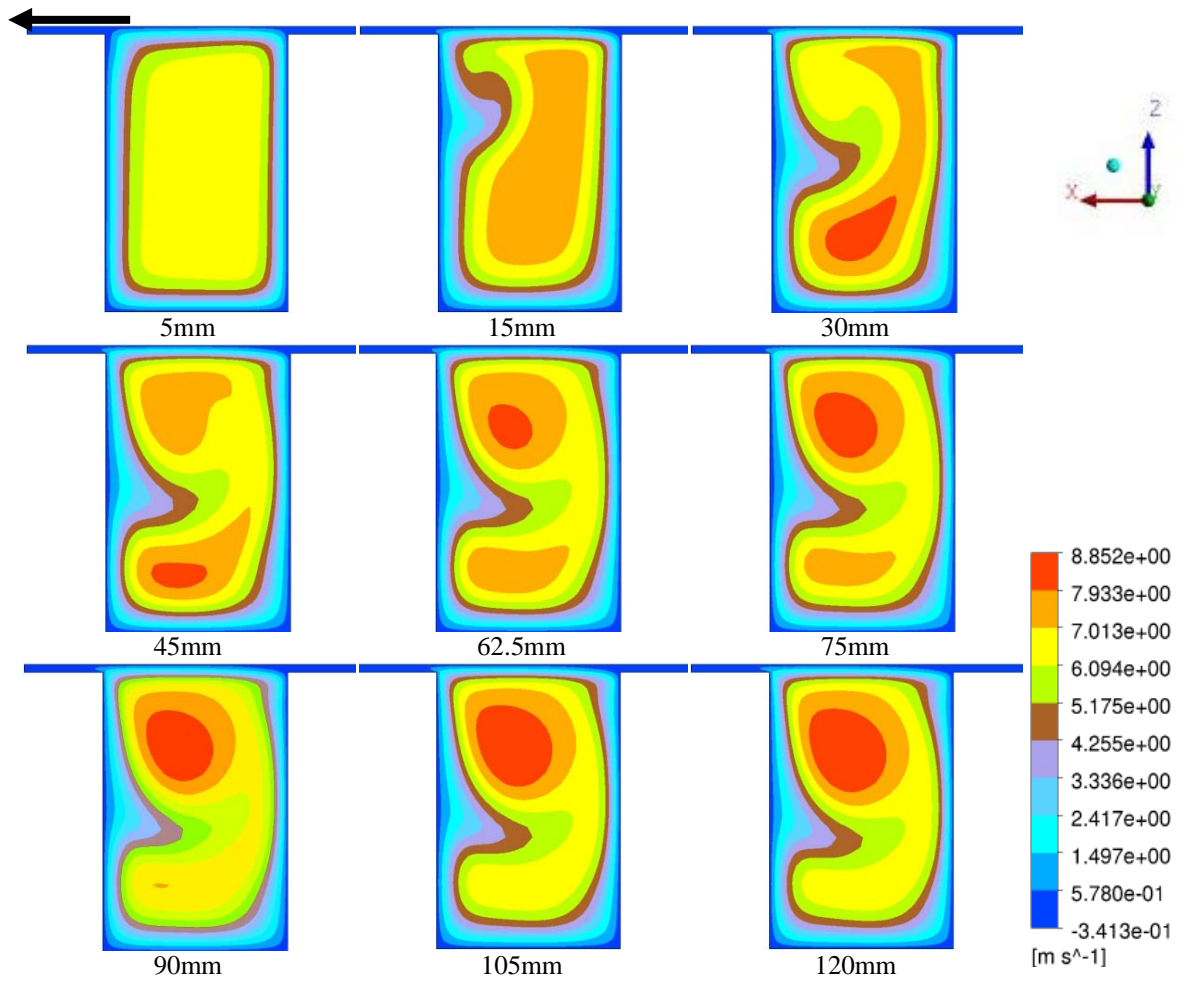
Figure 21:   *Radial Velocity at different locations inside the groove of the rotor, RPM=750 & ΔP=50kPa*

Figure 22 shows movement of fluid particle from the bottom to the top, fluid particle located near the bottom wall do not show such movement rather it goes straight towards the periphery with very slight change in direction near the midplane.
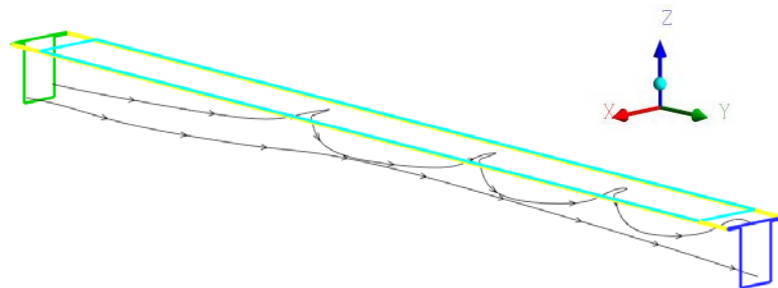
Figure 22:   *Tracing of fluid particle at the top and bottom of the rotor groove.*

3D Streamline plots of velocity in the groove is good indicator of swirling motion at the top, radial transportation of fluid in the bottom of the groove and movement of the fluid streams from bottom to top, figure 23.
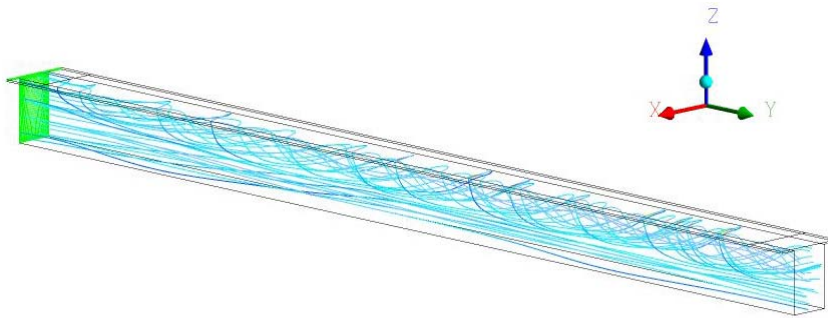
Figure 23:   *3D Streamlines in the rotor, rotational motion in the top part of groove and fairly radial motion in the bottom of the groove.*

5.3.1.2 Z- velocity

Z-Velocity is responsible for the rotation or creation of swirl in the fluid. Figure 24 shows that in half of the groove z-velocity is in positive z direction and in the other half it is in negative z direction. Magnitude of z-velocity in positive and in negative z direction increases steadily as the fluid moves towards the periphery. Development of the red region near the right wall of groove and the growth of the blue region near left wall shows the increase in magnitude of z-velocity as the fluid moves towards the periphery. Flat plate is moving in the positive x direction, which results in a very high velocity in negative z direction near the left wall. Rotational motion is present mainly in the top part; flow in the bottom of groove remains unaffected to some extent. This can also be seen figure 23 where major change in the velocity is taking place only in the top portion of groove.
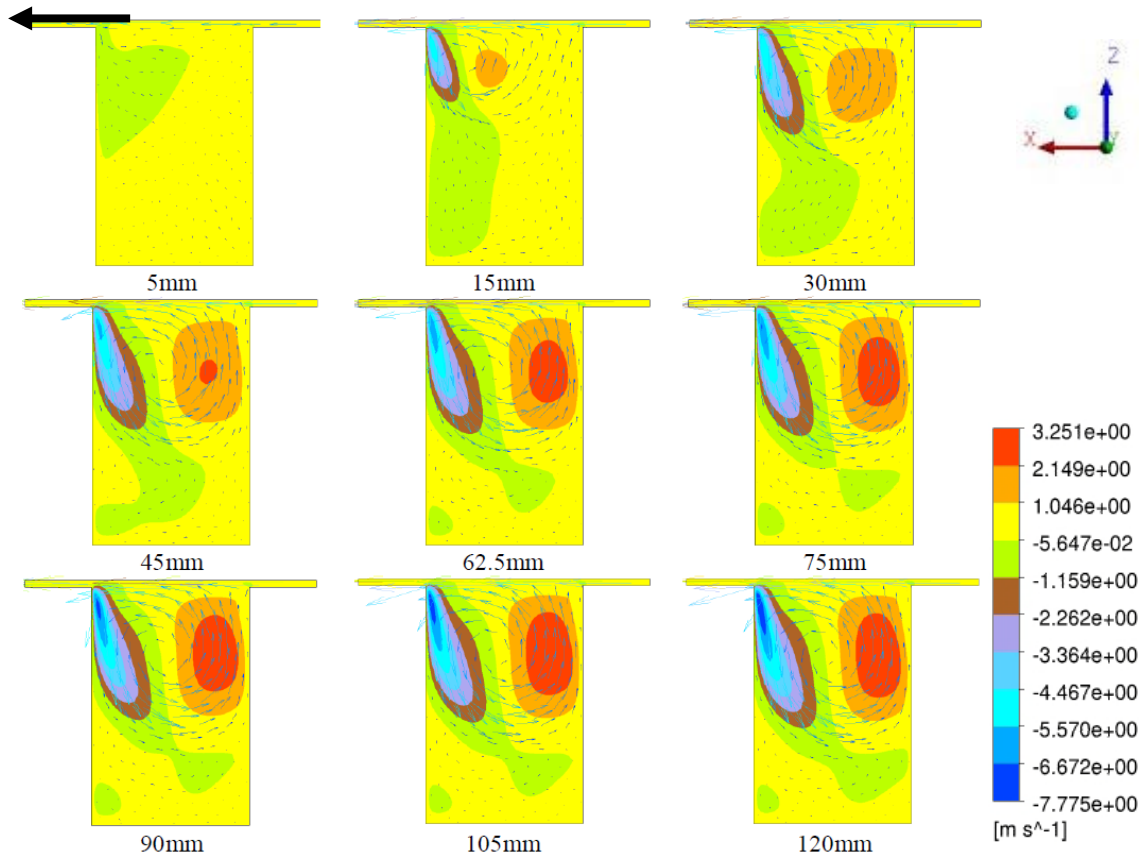
Figure 24: *The z-velocity in the rotor groove at different cross sections along the groove with vectors indicating flow direction, RPM=750 & ΔP=50kPa*

5.3.2 Flow in the stator

The flow in the stator is governed by the pressure difference. Plots below indicate the components of velocity in the stator of refiner at various cross sections along the groove. Flow in the stator is going towards the origin (negative y-direction).

5.3.2.1 Y- velocity

The y-velocity is strong in the rotating flow (primary vortex) that is developed in the top portion of the groove. Magnitude of y-velocity in the primary vortex decreases as the fluid moves towards the origin and it increases in the bottom of the groove. This is exactly opposite to what was observed in the case of rotor, but the pattern of the flow is almost the same in both the rotor and the stator. Change in flow pattern in the stator groove at different cross section is less evident as compare to rotor, in rotor flow condition changes at almost every cross section.

Figure 25: *Y- Velocity in the stator groove at different cross sections,*
ΔP=50kPa, RPM =750
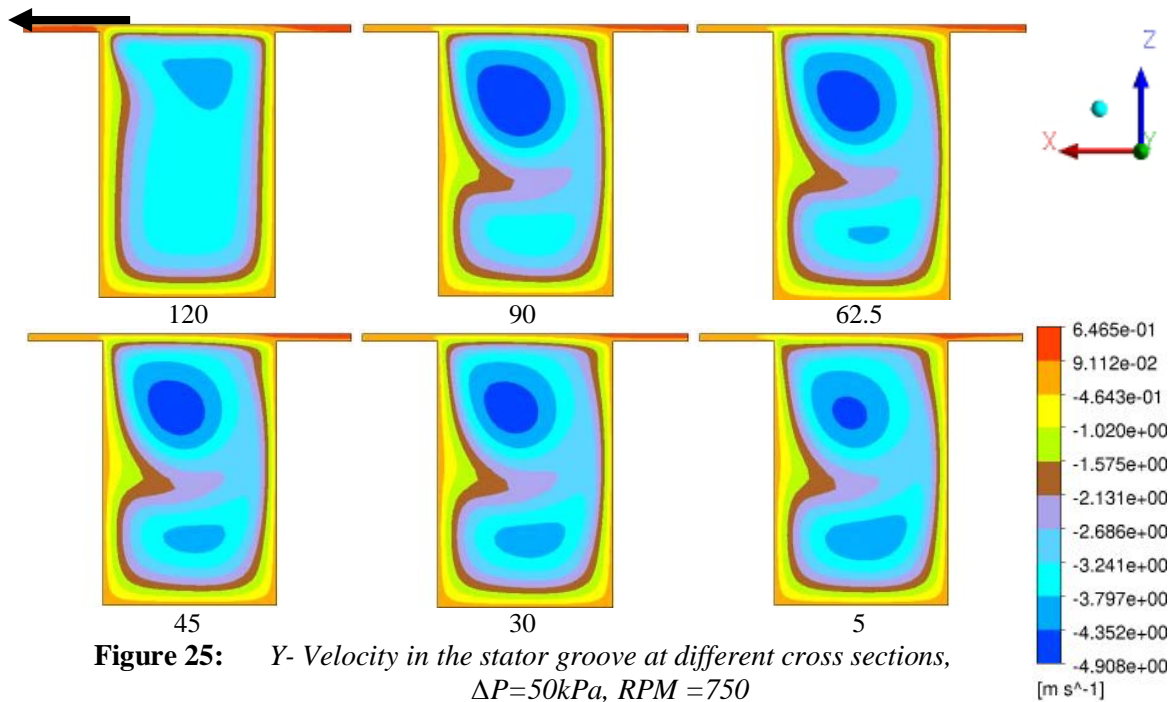
5.3.2.2 Z-velocity

The z-velocity creates a rotational motion in the groove, at the start of groove rotational motion is very strong but it decreases gradually as the fluid moves towards the origin. The z-velocity in stator is comparatively higher than the rotor, but in case of stator there is very little transportation of fluid at the bottom of the groove, flow is pre dominantly present only at the top of the groove. The vectors indicate the flow direction. It is also evident from the vector plot that the flow is mainly present in the top of the groove.
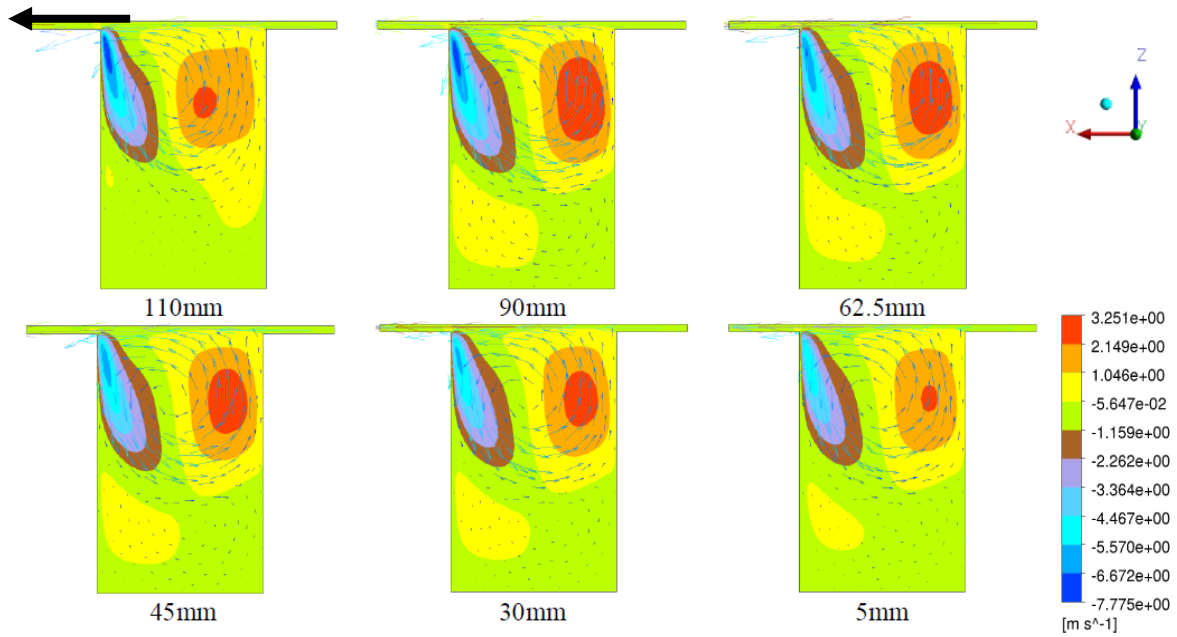
Figure 26: *Z-velocity plot at different cross section along the stator groove with vectors indicating the flow direction, ΔP=50kPa, RPM =750.*

Streamlines plot through the stator groove are good indicators of rotational or swirling motion at the top and fluid transportation along groove in the bottom.
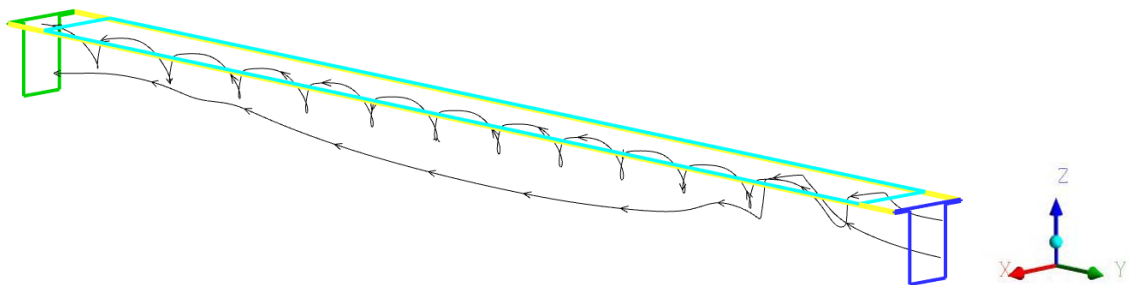
Figure 27: *Fluid particle tracing at the top and bottom of stator groove going in the negative Y-direction*

Streamline at the top of the groove shows very high rotational velocity and the one at the bottom shows that fluid particle has some rotation initially but afterwards it follows a straight path to the origin. A complete image of 3D streamline through stator groove is shown in figure 28
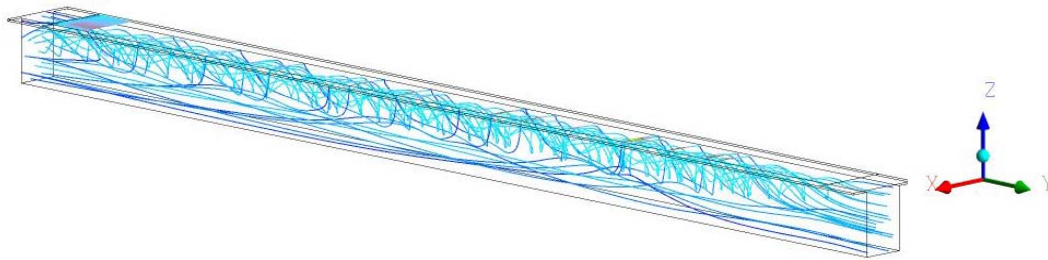
Figure 28: *3D Streamlines through the stator groove, higher rotational motion at the top. Streamlines going in the negative Y-direction towards the origin.*

5.3.3 Comparison of the flow in the rotor and the stator

Streamline plot in the rotor groove shows the formation of three vortices. A relatively bigger vortex is present in top portion of the grooves and two smaller vortices are in the bottom of the groove as shown in figure 29.

Figure 29: *Vector plot (left) and streamline plot (right) at midplane (62.5mm) in the rotor*

In the stator surface streamline (see figure 30) plot shows formation of two vortices. This is slightly different from the streamline plot of rotor (figure 29) where there is more rotation in the bottom. This may be due to the presence of coriollis force in the rotor model.

Figure 30: *Vector plot (left) and streamline plot (right) at midplane (62.5mm) in the stator.*

Appendix C consist of streamline close to the bar edge in the rotor and in the stator at different pressure differences and refiner speed.

5.3.4 Flow in the gap

In this section fluid flow in the narrow region between the rotating and stationary disc is analyzed. Flow inside the gap is very significant; most of the refining take places in this narrow region see section 2.2. Fibres are stapled on the bar region of rotor and stator and get treated due to motion of rotating disc. Fibre length is increased due to the shear force applied by the moving plate, or fibres got cut and shorten as one bar approaches the other bar. These flocs of fibres that are stapled on the bar region of rotor may break loose and may become a part of inward flow in the stator (and may become stapled again), or become part of the outward rotor flow [9].

5.3.4.1 Static pressure variation in gap

Static pressure variation is very prominent in the gap and in the region close to it. As the moving bar approaches the stationary bar, the static pressure increases, and as it moves away, the pressure value start to decrease. In figure 31, pressure is plotted in the gap for two different RPM i.e.750 & 900 and a pressure gradient of 50kPa, at a cross section located at the midplane (62.5mm), the flat plate is moving in positive x-direction. An increase in pressure gradient across the rotor will increase the value of static pressure.
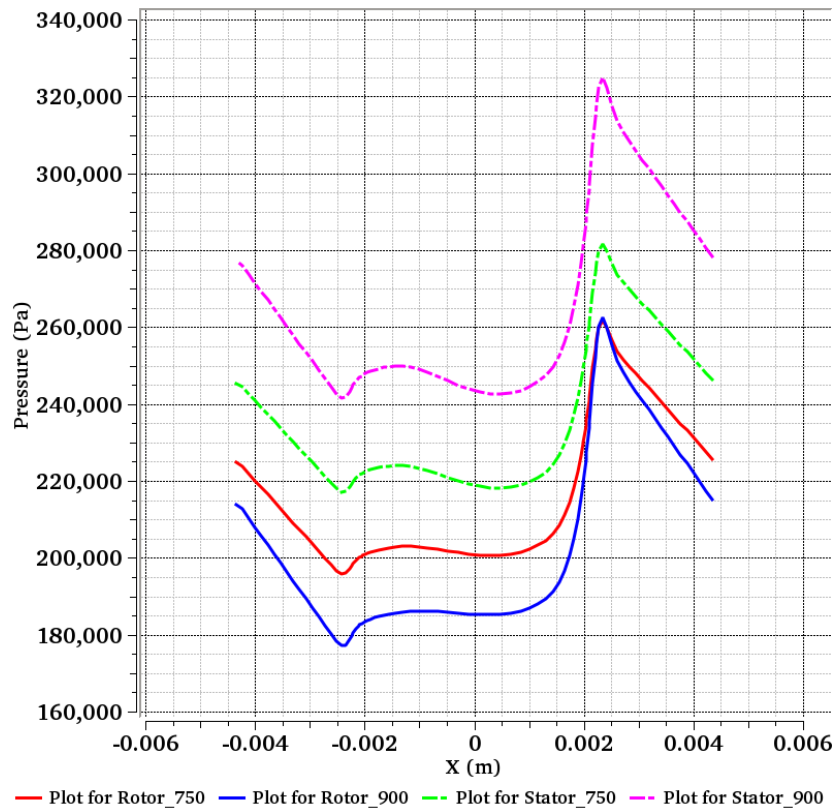
Figure 31: *Static pressure in Rotor Gap at a cross section located at 62.5mm (midplane) for refiner speed of 750 & 900 RPM and ΔP=50KPa.*

In figure 31, it can be seen that the static pressure is smaller in the middle region of the groove and as the rotating bar approaches the stationary bar there is a rapid increase in static pressure. From 0 to 2.5mm, the static pressure increases from around 202 kPa to 263 kPa and from 185kPa to 263 kPa for the rotor speed of 750 and 900 respectively. This rapid rise in pressure increases the intensity of refining on the fibres that are stapled on the bar edge.

As mentioned earlier that in the stator fluid velocity is smaller as compared to the rotor, so the pressure in the stator is higher than the rotor. Peak pressure values as the bar approaches the stationary bar are higher in this case.

5.3.5 Rotational motion
Inside a gap, there is small region in which rotational velocity of fluid increases as the rotating bar crosses the stationary bar.
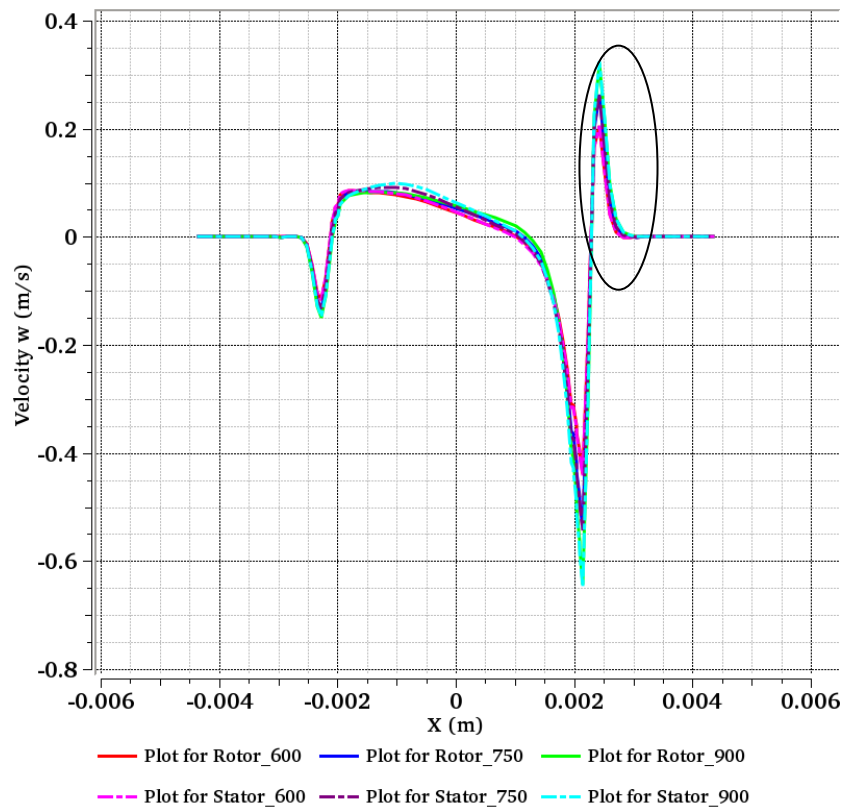
Figure 32: *Rotational Motion in the gap at the midplane for RPM 600,750 &900 and ΔP=50KPa*

In figure 32, the rotating bar is moving in the positive x direction, and the gap start from 2.35mm. This increase in rotational velocity is localized to a very small region, after which it decreases

5.4 Strain rate

Strain rate is important to determine, as it shows where the refining work is being applied on the fibers and the intensity of refining. Strain rate plots shows very small amount of work in the groove of rotor and stator, almost all the work is being done in the gap region. This phenomenon enhances the importance of flow in the gap. In order to find out the shear force applied on the fiber, strain rate was calculated on a surface area equivalent to the size of a fiber i.e. around 2mm long and 0.4mm wide. Value of the strain rate was integrated over that surface.

It is assumed that a fiber is hanging on the bar edge and half of the fiber is lying on the bar and other half is hanging vertically, resulting in a shear force applied in the

horizontal and vertical direction as shown in figure 33. Table 7 gives the strain rate and shear force on the fiber in the rotor of the refiner.
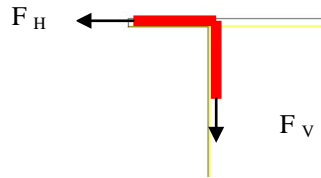

Figure 33:   *Fibre stapled on the bar edge*

Where F_H, is the horizontal force acting on the fibre stapled at the bar edge, this force is due to the motion of the flat plate and F_V is the vertical force acting on the fibre stapled at the bar edge, this force is due the motion of fluid down into the groove.

	RPM	ΔP	Integral Strain-Horizontal (m^2/s)	Integral Strain-vertical (m^2/s)	Shear Force-Horizontal (N)	Shear Force-vertical (N)
R	750	50	12.08	7.56	1.208	0.76
R	750	75	12.07	7.51	1.207	0.75
R	750	100	12.05	7.47	1.205	0.74
R	900	50	14.89	9.35	1.489	0.94
R	900	75	14.86	9.26	1.486	0.93
R	900	100	14.84	9.18	1.484	0.92

Table 7:   *Strain rate and shear force on the fibre in rotor*

For Newtonian fluids, the shear force is a product of viscosity and shear strain rate. Using this relation, the force the fibre is subjected to can be calculated as mentioned in table 7. It shows that shear force increases with the increase in speed of refiner; pressure change has a very little impact on the fibre.

In the groove the strain rate does not change; it changes in the gap and in the region close to the wall located in the direction of rotation of flat plate (positive x-direction). To measure that, strain rate was plotted in the gap and in the region close to wall; Data sampling was done on the lines shown in the figure 34. Line inside the gap is located at (z= 3.52mm) and the line in the groove near the left wall is located at (x = 2.33mm).
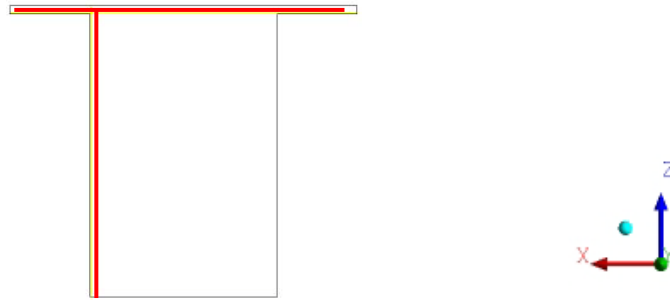
Figure 34: *Location at which strain rate is measure, flat plate rotating in positive x-direction.*

Figure 35 shows the rapid increase in the strain rate, as the rotating bar approaches the stationary bar, this increase in the value of the strain rate is for a short duration but it has a profound impact on the fibres that are stapled on the edge of bar. The shear force that is being applied on the fibre can result in fibre elongation, cutting of the fibre, production of fines etc.
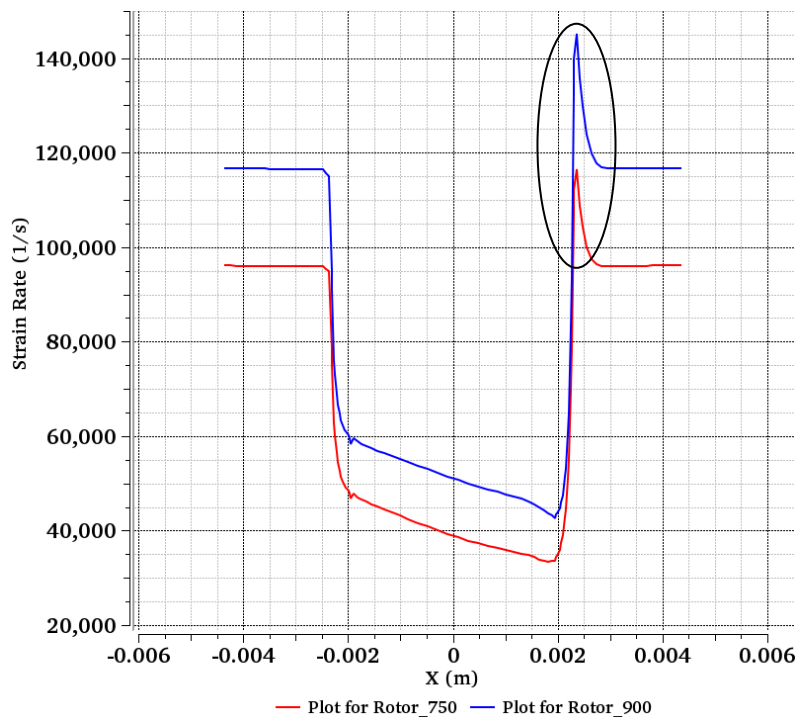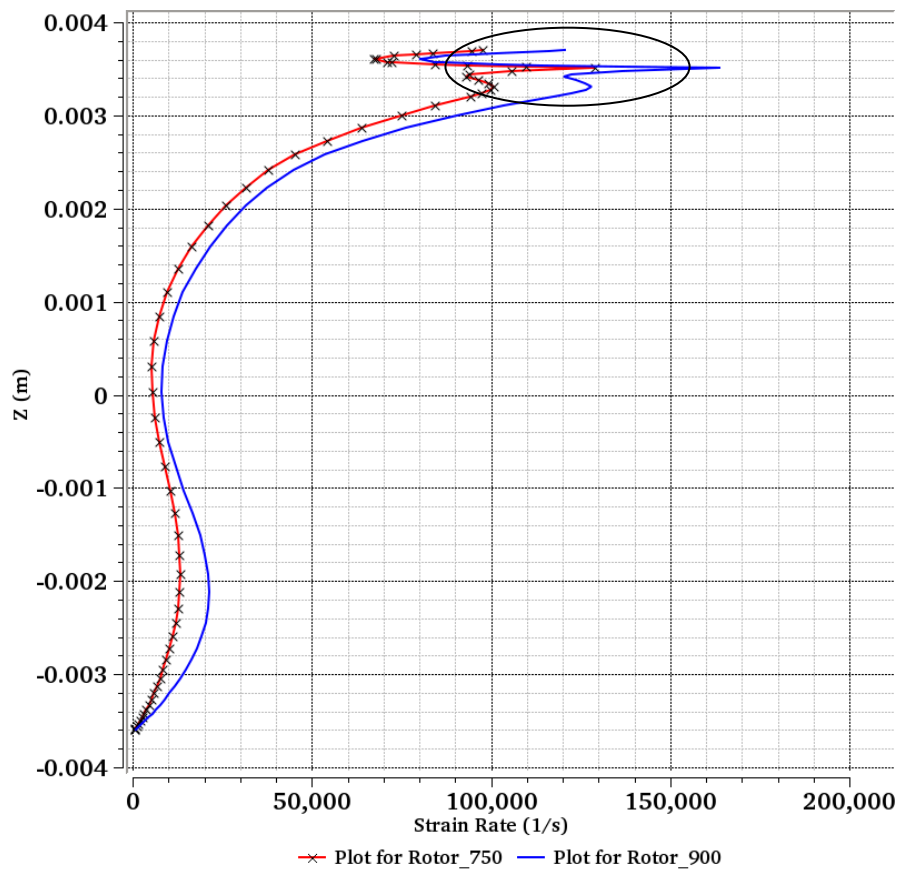

Figure 35: *Strain rate in the gap for refiner speed of 750(red) and 900 (blue) at a cross section located at midplane (62.5mm).*

Figure 36 is the plot of strain rate in along the left wall of the groove. Shear force in the vertical direction is due to this strain rate. This shear force is produced due to downward motion of the fluid along the wall of the groove. As the flat plate rotates it takes fluid with it, very small amount of the fluid will go into the gap and most of the fluid will move down into the groove, which results in increased strain rate and shear force on the fibers hanging at the bar edge. Horizontal and vertical forces acting on the fibre can alter the fibre structure and mechanical properties of the fibre.

Figure 36 shows an increase in the strain rate in the top half of the groove. Near the bar edge i.e. at z = 3.3mm to 3.7mm, strain rate at this location is high as compare to the rest of the groove.

Variation of the strain rate at different cross sections along the rotor groove is shown Appendix B.

Figure 36: *Strain rate near the left wall of groove for refiner speed of 750 (red) and 900 (blue) at a cross section located at midplane (62.5mm.*

6 Conclusion & future work

In this study flow development inside the rotor and the stator groove and the flow in the gap is analyzed. From the numerical results following conclusions can be drawn. It also includes recommendation for future work

- Fluid flow in the rotor depends on the pressure difference and on the speed of the refiner. Higher pressure difference reduces the flow rate in the rotor.
- Fluid flow in the stator depends on pressure difference; higher pressure difference increases the flow rate through the stator.
- Transportation of the fluid is along the groove. In the model studied it is in y-direction. Flow velocities in y-direction are comparatively higher in magnitude as compare to the flow velocities in x and z direction.
- Flow inside the gap i.e. narrow region between the rotating flat plate and groove is subject to higher static pressure, high rotational motion and high shear force. In an actual disc refiner flocs of fibre are present in this gap. Higher pressure and shear force contribute to the refining of the fibre. It can alter the fibre structure and its mechanical properties. Change in fibre properties can be the desired or undesired one. In order to find out the conditions under which maximum desired properties can be achieved a multiphase analysis is required in which individual fibre can be studied and analyzed.
- Strain rate and shear force studied in this study is mainly due to the rotation of flat plate, shear force present due to individual fibers is not considered. It is not yet clear that how much refining is due to fibre to fibre interaction.
- Strain rate in the groove is constant, it only varies in the gap and in the region close to it (See Appendix A)
- Streamline plots shows the formation of three vortices in case of rotor groove and two in case of stator groove. The difference may be due to the presence of the coriollis force in the rotor.
- Rotational motion is present both in the rotor and in the stator, 3D streamlines plots and z-velocity plots shows that rotation is strong in the top half of stator

groove as compare to the rotor groove. In the bottom of the stator groove fluid has very little rotation and it goes straight toward the origin (see figure 31).

- Rotational motion increases in the rotor as the fluid moves towards the periphery. Rotational motion is strong in the top portion of the groove. In the bottom of the groove fluid start to rotate towards the end (see figure 24).

- In the current study a single groove model is considered. It would be interesting to simulate the fluid motion in the complete sector containing multiple bars and grooves.

- Different multiphase model with non Newtonian fluid can be analyzed using different type of particle shapes.

- Flow inside the gap can be further analyzed by studying effect of gap size on the refining work.

- In an actual disc refiner grooves are usually at a small angle, effect of angle on the development of flow inside the groove and gap can be studied as it will be more close to the actual geometry.
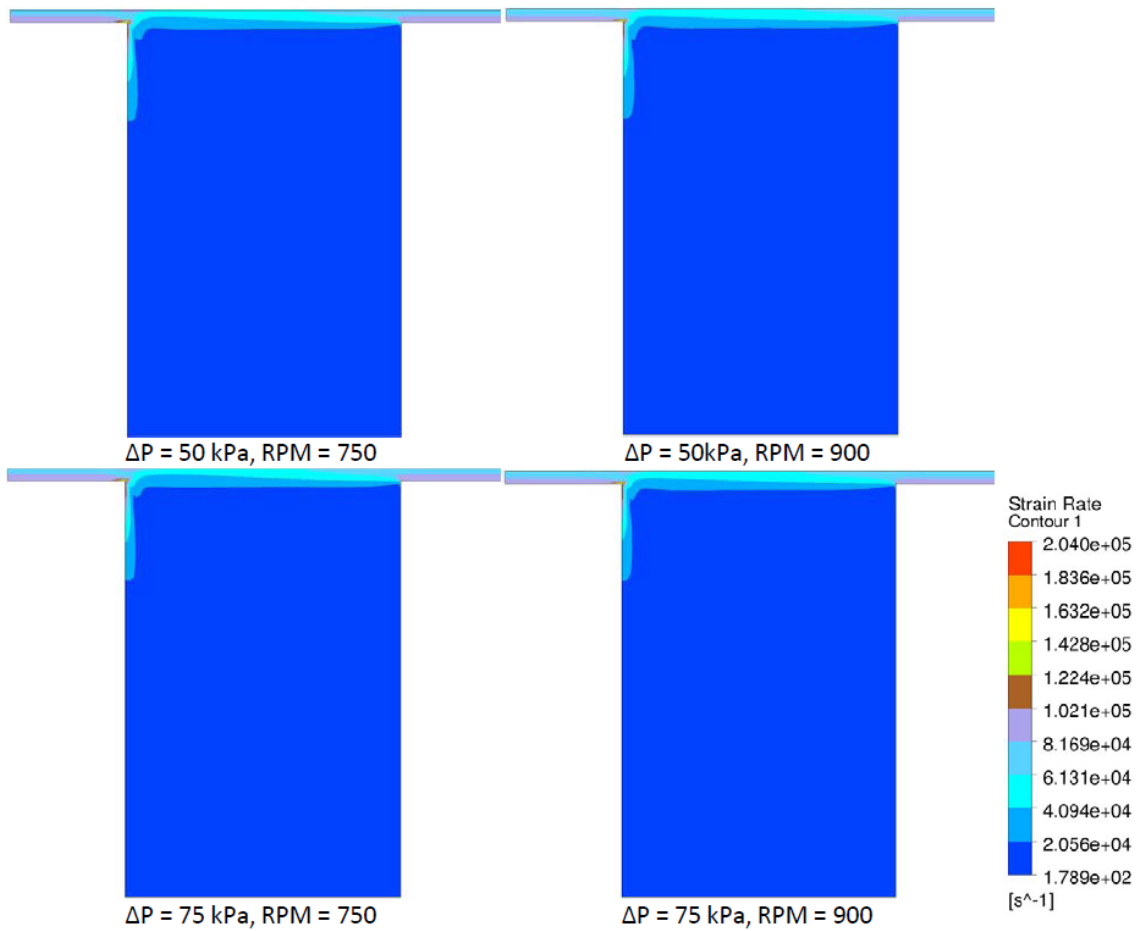
7 References

[1]   Wadood, H, Cellulosic materials: fibers, networks and composites, Mechanical pulping Page 57.

[2]   KANO, T., IWAMIDA, T. and SUMI, Y. (1982). Energy Consumption in Mechanical Pulping. Pulp & Paper Magazine Canada, 83(6), T157-T161.

[3]   Vena, P.F, Thermomechanical pulping, chemi-thermomechanical pulping and Bio-Thermomechanical pulping of bugweed and Pinus Patula.

[4]   Lumiainen,J, Refining of chemical pulp, Papermaking Science and Technology,Papermaking Part 1, Stock Preparation and Wet End, Book 8, Fapet Oy, H. Paulapuro(Ed.), Gummerus Printing, Jyväskylä, Finland, 2000, 87-121.

[5]   Sundholm, J. (1999) What is mechanical pulping, Papermaking Science and Technology, Book 5.

[6]   Waterhouse,J.F, Whither Refining?: Refining 97, 4th International refining Conference, March 18-20,1997;Plazzo Della Fonte, Fiuggi, Italy.

[7]   Technical marketing programme (TEMAP), CANFOR Pulp refining seminar Part II: Selected Topics.

[8]   Norman, B. (ed), 1992, *Pappersteknik*, Department of Pulp and Paper Chemistry and Technology, Division of Paper Technology, Royal Institute of Technology, Stockholm

[9]   Fox, T. S., 1980, *Inside a Disk Refiner*, International Symposium on the Fundamentals Concepts of Refining, pp. 281-313

[10]   Versteeg, H.K and Malalasekera,W: An introduction to computational fluid dynamics-The finite volume method (second edition).

[11]   Pope, S.B, Turbulent Flows Cambridge (2000): Chapter 6- The scale of turbulent motion.

[12]   Henningson, Dan and Berggren,M, Fluid Dynamics (2005): Theory and Computation, Chapter 2-Flow Physics.

[13]   Wallin, Stefen: Lecture notes on Turbulence modelling (2011) at Royal Institute of Technology (KTH).

[14]   ANSYS FLUENT 13.0 Documentation, ANSYS, Inc.

[15]   Loijas, M, Factors effecting axial forces on low consistency refining. Tampere University of Applied sciences,Finland.

[16]   Björkman,M, Numerical Modelling of flow in Refiner (2010), Royal Institute of Technology (KTH),Stockholm, Sweden and Innventia AB, Stockholm.

[17]   Eriksen,O and Hammar, L.A, Refining mechanism and development of TMP properties in low consistency refiner.

[18]   Scolofsky, S, Lecture notes on Fluid dynamics for ocean and environmental engineering (OCEN 678) at Texas A&M university, Texas, USA.
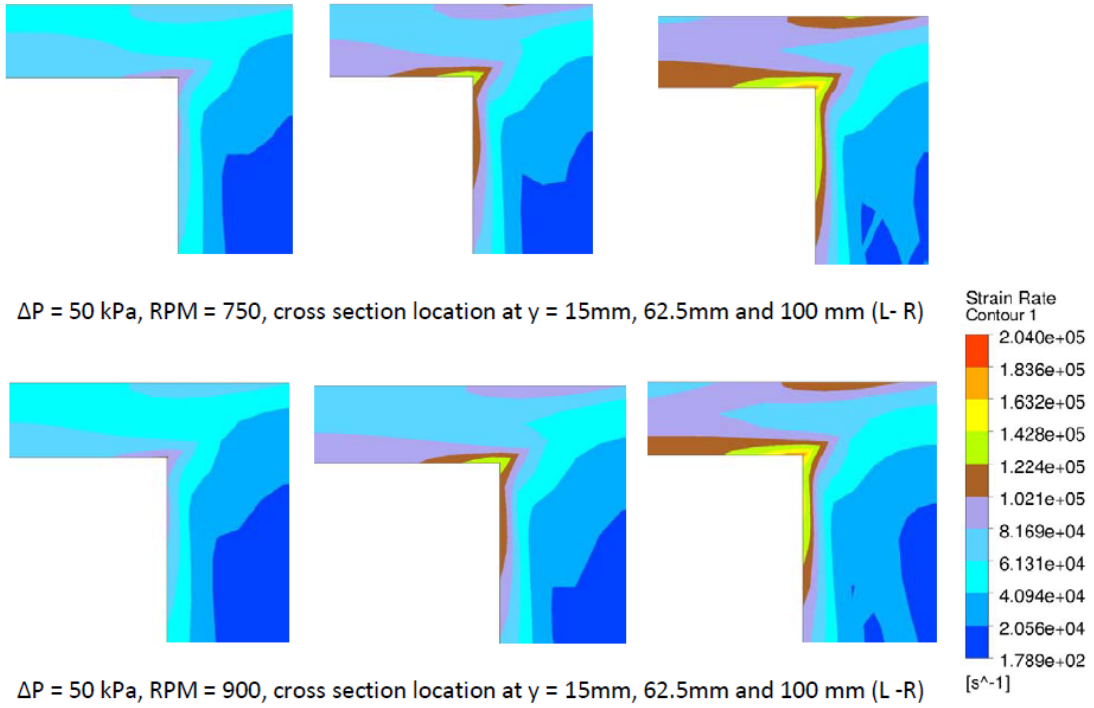
Appendix A

This shows the variation of the strain rate in the gap and in the region close to the gap. Strain rate is present only in the gap and in the rest of the groove it is constant.

ΔP = 50 kPa, RPM = 750   ΔP = 50kPa, RPM = 900

ΔP = 75 kPa, RPM = 750   ΔP = 75 kPa, RPM = 900

Strain Rate
Contour 1
2.040e+05
1.836e+05
1.632e+05
1.428e+05
1.224e+05
1.021e+05
8.169e+04
6.131e+04
4.094e+04
2.056e+04
1.789e+02
[s^-1]

Appendix B

This shows the variation of the strain rate in the gap at different cross sections along the rotor groove. Strain rate increases as the fluid moves towards the periphery. Strain rate is high at 100mm.


ΔP = 50 kPa, RPM = 750, cross section location at y = 15mm, 62.5mm and 100 mm (L- R)

ΔP = 50 kPa, RPM = 900, cross section location at y = 15mm, 62.5mm and 100 mm (L -R)

Strain Rate
Contour 1
2.040e+05
1.836e+05
1.632e+05
1.428e+05
1.224e+05
1.021e+05
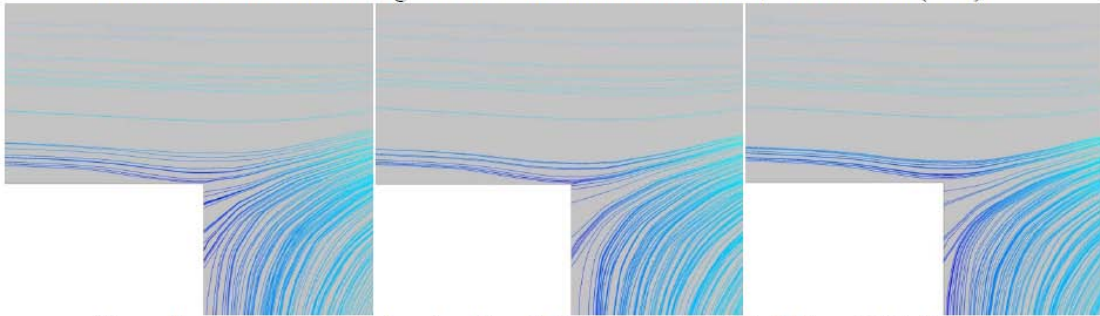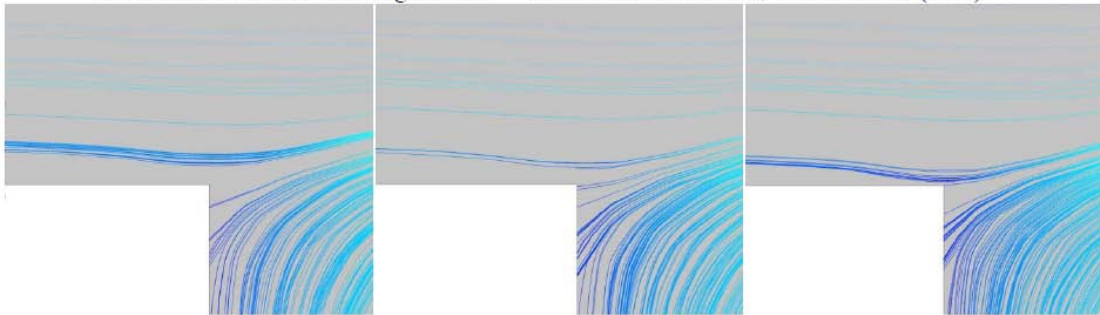8.169e+04
6.131e+04
4.094e+04
2.056e+04
1.789e+02
[s^-1]

Appendix C

This shows the surface streamlines near the bar edge in the rotor and in the stator groove for the different pressure differences and the refiner speed.

ROTOR
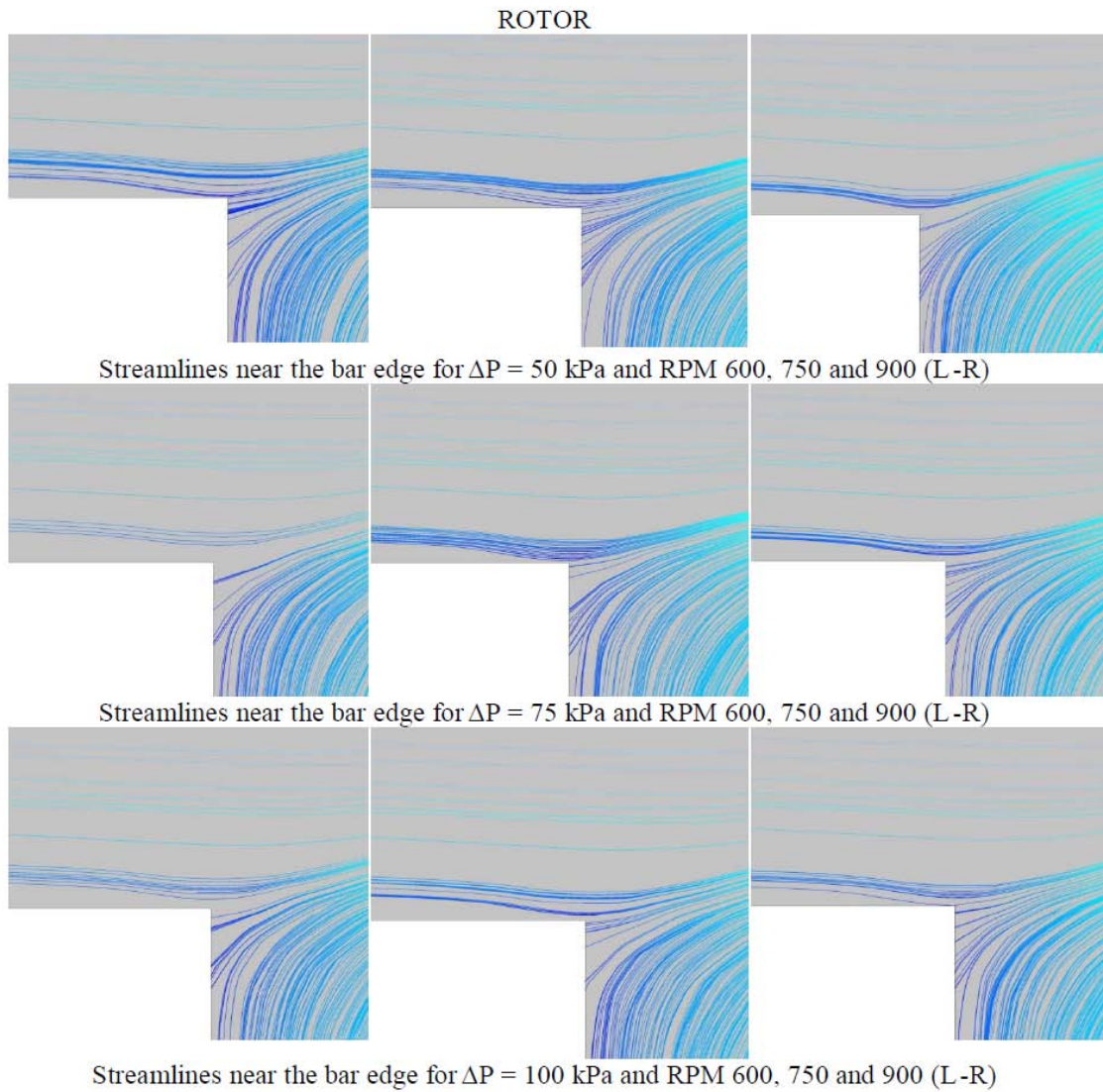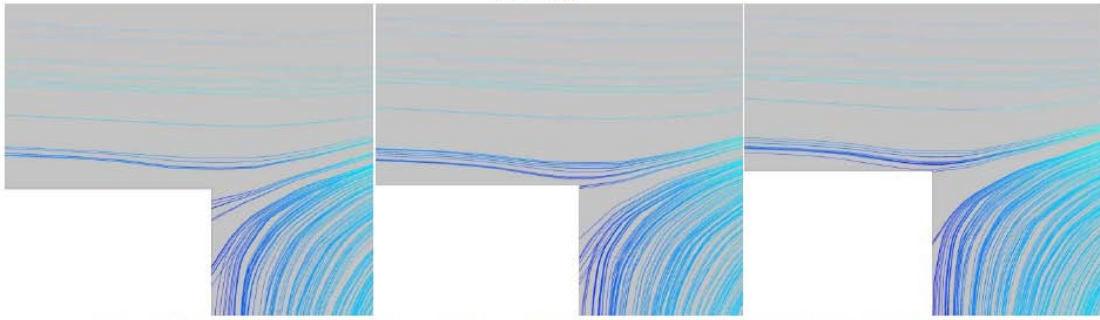
Streamlines near the bar edge for $\Delta P = 50$ kPa and RPM 600, 750 and 900 (L-R)

Streamlines near the bar edge for $\Delta P = 75$ kPa and RPM 600, 750 and 900 (L-R)

Streamlines near the bar edge for $\Delta P = 100$ kPa and RPM 600, 750 and 900 (L-R)

STATOR

Streamlines near the bar edge for ΔP = 50 kPa and RPM 600, 750 and 900 (L -R)

Streamlines near the bar edge for ΔP = 75 kPa and RPM 600, 750 and 900 (L -R)

Streamlines near the bar edge for ΔP = 100 kPa and RPM 600, 750 and 900 (L-R)